REPORT DOCUMENTATION PAGE

1a. REPORT SECURITY CLASSIFICATION Unclassified	1b. RESTRICTIVE MARKINGS
2a. SECURITY CLASSIFICATION AUTHORITY	3. DISTRIBUTION/AVAILABILITY OF REPORT Approved for public release; distribution is unlimited.
2b. DECLASSIFICATION/DOWNGRADING SCHEDULE	
4. PERFORMING ORGANIZATION REPORT NUMBER(S)	5. MONITORING ORGANIZATION REPORT NUMBER(S)
6a. NAME OF PERFORMING ORGANIZATION Naval Postgraduate School 6b. OFFICE SYMBOL (*If applicable*) 34	7a. NAME OF MONITORING ORGANIZATION Naval Postgraduate School
6c. ADDRESS (*City, State, and ZIP Code*) Monterey, CA 93943-5000	7b. ADDRESS (*City, State, and ZIP Code*) Monterey, CA 93943-5000
8a. NAME OF FUNDING/SPONSORING ORGANIZATION 8b. OFFICE SYMBOL (*If applicable*)	9. PROCUREMENT INSTRUMENT IDENTIFICATION NUMBER
8c. ADDRESS (*City, State, and ZIP Code*)	10. SOURCE OF FUNDING NUMBERS Program Element No. / Project No. / Task No. / Work Unit Accession Number

11. TITLE (*Include Security Classification*)
A NUMERICAL STUDY OF DYNAMIC CRACK PROPAGATION IN COMPOSITES

12. PERSONAL AUTHOR(S) Erol Babiloglu

13a. TYPE OF REPORT	13b. TIME COVERED	14. DATE OF REPORT (*year, month, day*)	15. PAGE COUNT
Master's Thesis	From To	September, 1992	78

16. SUPPLEMENTARY NOTATION
The views expressed in this thesis are those of the author and do not reflect the official policy or position of the Department of Defense or the U.S. Government.

17. COSATI CODES			18. SUBJECT TERMS (*continue on reverse if necessary and identify by block number*)
FIELD	GROUP	SUBGROUP	dynamic fracture of composites

19. ABSTRACT (*continue on reverse if necessary and identify by block number*)

A numerical study was performed to investigate the dynamic crack propagation in fibrous composite plates utilizing the finite element method. A rectangular plate of uniform thickness, which had a propagation central crack, was used for the study. The plate was unidirectional composite panel and the load was applied in the longitudinal direction of the composite plate. Fracture energies were calculated for given speeds of cracks. The objective of the study was to examine the effect of different composite material properties, crack speeds, and densities on the fracture energy. The discontinuous node-release tecnique was used to model the crack propagation.

The numerical study showed that the fracture energy was higher for a lower elastic modulus ratio, if all other conditions were held the same. Furtermore, a lower crack propagation velocity or a lower material density resulted in a higher fracture energy, respectively, provided the rest of the parameters held constant.

20. DISTRIBUTION/AVAILABILITY OF ABSTRACT	21. ABSTRACT SECURITY CLASSIFICATION	
☒ UNCLASSIFIED/UNLIMITED ☐ SAME AS REPORT ☐ DTIC USERS	Unclassified	
22a. NAME OF RESPONSIBLE INDIVIDUAL Young W. Kwon	22b. TELEPHONE (*Include Area code*) (408) 646-3385	22c. OFFICE SYMBOL ME/kw

DD FORM 1473, 84 MAR 83 APR edition may be used until exhausted
All other editions are obsolete

Approved for public release; distribution is unlimited.

A Numerical Study of Dynamic Crack Propagation in Composites

by

Erol Babiloglu
Lieutenant(j.g.) Turkish Navy
B.S., Turkish Naval Academy, 1985

Submitted in partial fulfillment
of the requirements for the degree of

MASTER OF SCIENCE IN MECHANICAL ENGINEERING

from the

NAVAL POSTGRADUATE SCHOOL
September, 1992

ABSTRACT

A numerical study was performed to investigate the dynamic crack propagation in fibrous composite plates utilizing the finite element method. A rectangular plate of uniform thickness, which had a propagating central crack, was used for the study. The plate was a unidirectional composite panel and the load was applied in the longitudinal direction of the composite plate. Fracture energies were calculated for given speeds of cracks. The objective of the study was to examine the effect of different composite material properties, crack speeds, and densities on the fracture energy. The discontinuous node-release technique was used to model the crack propagation.

The numerical study showed that the fracture energy was higher for a lower elastic modulus ratio, if all other conditions were held the same. Furthermore, a lower crack propagation velocity or a lower material density resulted in a higher fracture energy, respectively, provided the rest of the parameters held constant.

TABLE OF CONTENTS

ACKNOWLEDGEMENTS

I would like to express my sincere thanks and gratitude to all of the instructors and the staff in the Naval Engineering Curriculum, especially to Professor Young W. Kwon for their patience, guidance, and technical support throughout this research.

The great love and encouragement that I received from my wife, Erva, and from our parents were key points to being successful. Additionally, the joyful energy we received as parents from our daughter, Sena, was an important factor both for us during this period of study in the United States. Thank you, Erva, for being a trustworthy and competent wife; your willingness to accompany me here from Turkey brought happiness too great for explanation.

I. INTRODUCTION

Dynamic fracture deals with problems having a crack within a body where the inertial forces play an important role. The early investigation of the dynamic fracture analysis goes back to the case of unstable crack propagations in some ships during World War II. The dynamic fracture problems involve crack initiation and crack propagation. There are two principal types of problems. One is applying a dynamic load to a body containing stationary cracks, and the other is concerned about a body with a moving crack. The second type of problems can be classified into two different modes; propagation and generation modes.

Stationary crack problems involve cracks within structures that are subjected to dynamic loading, such as an impact load. For example, Chen performed a numerical analysis to find the dynamic stress intensity factor for a rectangular plate having a central crack. He used the finite difference technique and discussed the dynamic behavior of the stress intensity factor. He argued that the oscillations on the stress intensity versus time curve were mainly due to scattering phenomena from the crack tip and the boundary surfaces. He concluded that the overshooting of the dynamic stress intensity factor is attributed mainly to the geometry and loading.[Ref. 1]

The generation mode involves moving cracks expanding at prescribed rates. The main objective of the study is to compute the stress intensity factor or the fracture energy and to determine the fracture toughness. The propagation mode deals with the cases where fracture toughness is known. The objective is to predict the crack propagation and its arrest for a given load. One of useful models to investigate the crack propagation and arrest was the double cantilever beam. Kanninen and his coworkers [Ref. 2] proposed the model and studied it extensively. Some of studies in the dynamic fracture were listed in the references [Ref. 3-7].

Although there are many literatures available for the dynamic fracture of isotropic materials, the studies of composite materials are not so common. Some of the fracture studies of composites were shown in references [Ref.8-10].

This study considered a rectangular plate made of unidirectional composite and containing a central, moving crack subjected to a uniform tensile load. The finite element method utilizing bilinear rectangular elements was used for this study. A parametric study to compare fracture energies in composite plates for various conditions was conducted. Different elastic modulus ratios, crack velocities, and material densities were considered.

II. MATHEMATICAL DERIVATION

A. GOVERNING EQUATIONS

The governing equations for the problem of elasticity are equations of equilibrium, constitutive equations, and kinematic equations. For the two-dimensional problem, they are given below. Equations of equilibrium are

$$\begin{aligned} \frac{\partial \sigma_x}{\partial x} + \frac{\partial \tau_{xy}}{\partial y} - \rho \frac{\partial^2 u}{\partial t^2} = 0 \\ \frac{\partial \tau_{xy}}{\partial x} + \frac{\partial \sigma_y}{\partial y} - \rho \frac{\partial^2 v}{\partial t^2} = 0 \end{aligned} \qquad (1)$$

where σ_x, σ_y, and τ_{xy} are the two normal stresses in the x and y direction and the shear stress, respectively. ρ is the material density, and u and v are the displacements in the x and y direction, respectively. In addition, x and y are rectangular coordinate axes and t denotes time.

Constitutive equations are also known as stress-strain relations. The relations are given in a matrix form like

$$\{\sigma\} = [D]\{\epsilon\} \qquad (2)$$

where $\{\sigma\}$ and $\{\epsilon\}$ are, respectively, stress and strain vectors, that is

$$\begin{aligned} \{\sigma\} &= \{\sigma_x \quad \sigma_y \quad \tau_{xy}\}^T \\ \{\epsilon\} &= \{\epsilon_x \quad \epsilon_y \quad \gamma_{xy}\}^T \end{aligned} , \qquad (3)$$

and [D] is the material property matrix of size 3x3. For an isotropic material, the [D] matrices for plane stress and plane strain conditions, respectively, are

$$[D] = \frac{E}{(1-\upsilon)^2}\begin{bmatrix} 1 & \upsilon & 0 \\ \upsilon & 1 & 0 \\ 0 & 0 & \frac{1-\upsilon}{2} \end{bmatrix} \tag{4}$$

and

$$[D] = \frac{E(1-\upsilon)}{(1+\upsilon)(1-2\upsilon)}\begin{bmatrix} 1 & \frac{\upsilon}{1-\upsilon} & 0 \\ \frac{\upsilon}{1-\upsilon} & 1 & 0 \\ 0 & 0 & \frac{1-2\upsilon}{2(1-\upsilon)} \end{bmatrix} . \tag{5}$$

For a composite material, [D] matrix becomes

$$[D] = \begin{bmatrix} D_{11} & D_{12} & D_{13} \\ D_{21} & D_{22} & D_{23} \\ D_{31} & D_{32} & D_{33} \end{bmatrix} . \tag{6}$$

The details of Eq.(6) are shown in references.[Ref. 11]

Kinematic equations are also known as strain-displacement relations. The infinitesimal strains are expressed in terms of displacements as shown below:

$$\begin{Bmatrix}\epsilon_x\\ \epsilon_y\\ \gamma_{xy}\end{Bmatrix}=\begin{Bmatrix}\dfrac{\partial u}{\partial x}\\ \dfrac{\partial v}{\partial y}\\ \dfrac{\partial u}{\partial y}+\dfrac{\partial v}{\partial x}\end{Bmatrix} \tag{7}$$

B. BOUNDARY CONDITIONS

On the essential boundaries displacements u and/or v are prescribed, and on the nonessential or natural boundaries tractions are prescribed. Usually on a part of the boundary tractions are prescribed, while on the remainder of the boundary displacements are known. The tractions are given by

$$\begin{aligned}\Phi_x&=\sigma_x n_x+\tau_{xy} n_y\\ \Phi_y&=\tau_{xy} n_x+\sigma_y n_y\end{aligned} \tag{8}$$

where Φ_x and Φ_y are the tractions in x and y directions, respectively, and n_x and n_y are, respectively, the components of outward unit normal vector to the boundary.

Applying the method of weighted residual technique to the equations of equilibrium yields

$$\begin{aligned}I_1&=\int_\Omega\left(-\rho\frac{\partial^2 u}{\partial t^2}+\frac{\partial\sigma_x}{\partial x}+\frac{\partial\tau_{xy}}{\partial y}\right)\omega_1 d\Omega=0\\ I_2&=\int_\Omega\left(-\rho\frac{\partial^2 v}{\partial t^2}+\frac{\partial\tau_{xy}}{\partial x}+\frac{\partial\sigma_y}{\partial y}\right)\omega_2 d\Omega=0\end{aligned} \tag{9}$$

where ω_1 and ω_2 are test functions and Ω is the domain of a given problem. Applying the weak formulation results in

$$-\int_{\Omega}\begin{Bmatrix}\rho\dfrac{\partial^2 u}{\partial t^2}\omega_1+\sigma_x\dfrac{\partial\omega_1}{\partial x}+\tau_{xy}\dfrac{\partial\omega_1}{\partial y}\\ \rho\dfrac{\partial^2 v}{\partial t^2}\omega_2+\tau_{xy}\dfrac{\partial\omega_2}{\partial x}+\sigma_y\dfrac{\partial\omega_2}{\partial y}\end{Bmatrix}d\Omega+\int_{\Gamma}\begin{Bmatrix}\sigma_x n_x\omega_1+\tau_{xy}n_y\omega_1\\ \tau_{xy}n_x\omega_2+\sigma_y n_y\omega_2\end{Bmatrix}d\Gamma=0 \quad (10)$$

and Γ is the boundary of domain Ω. Rewriting Eq.(10) gives

$$\int_{\Omega}\left(\rho\begin{bmatrix}\omega_1 & 0\\ 0 & \omega_2\end{bmatrix}\begin{Bmatrix}\dfrac{\partial^2 u}{\partial t^2}\\ \dfrac{\partial^2 v}{\partial t^2}\end{Bmatrix}+\begin{bmatrix}\dfrac{\partial\omega_1}{\partial x} & 0 & \dfrac{\partial\omega_1}{\partial y}\\ 0 & \dfrac{\partial\omega_2}{\partial y} & \dfrac{\partial\omega_2}{\partial x}\end{bmatrix}\begin{Bmatrix}\sigma_x\\ \sigma_y\\ \tau_{xy}\end{Bmatrix}\right)d\Omega=\int_{\Gamma}\begin{Bmatrix}\Phi_x\omega_1\\ \Phi_y\omega_2\end{Bmatrix}d\Gamma \quad (11)$$

where

$$\int_{\Omega}\rho\begin{bmatrix}\omega_1 & 0\\ 0 & \omega_2\end{bmatrix}\begin{Bmatrix}\dfrac{\partial^2 u}{\partial t^2}\\ \dfrac{\partial^2 v}{\partial t^2}\end{Bmatrix}d\Omega \quad (12)$$

$$\int_{\Omega}\begin{bmatrix}\dfrac{\partial\omega_1}{\partial x} & 0 & \dfrac{\partial\omega_1}{\partial y}\\ 0 & \dfrac{\partial\omega_2}{\partial y} & \dfrac{\partial\omega_2}{\partial x}\end{bmatrix}\begin{Bmatrix}\sigma_x\\ \sigma_y\\ \tau_{xy}\end{Bmatrix}d\Omega \quad (13)$$

and

$$\int_{\Gamma}\begin{Bmatrix}\Phi_x\omega_1\\ \Phi_y\omega_2\end{Bmatrix}d\Gamma \quad (14)$$

are the mass matrix, stiffness matrix, and load vector, respectively.

A finite element discretization is applied to the domain and the following matrices are computed at the element domain.

C. MASS MATRIX

The mass matrix is given by

$$\int_{\Omega^e} \rho \begin{bmatrix} \omega_1 & 0 \\ 0 & \omega_2 \end{bmatrix} \begin{Bmatrix} \frac{\partial^2 u}{\partial t^2} \\ \frac{\partial^2 v}{\partial t^2} \end{Bmatrix} d\Omega \ . \qquad (15)$$

In this study both bilinear rectangular and linear triangular elements will be used to produce the finite element mesh. First the finite element derivation will be shown in detail using the bilinear rectangular element. The rectangular element is shown in Figure 1.

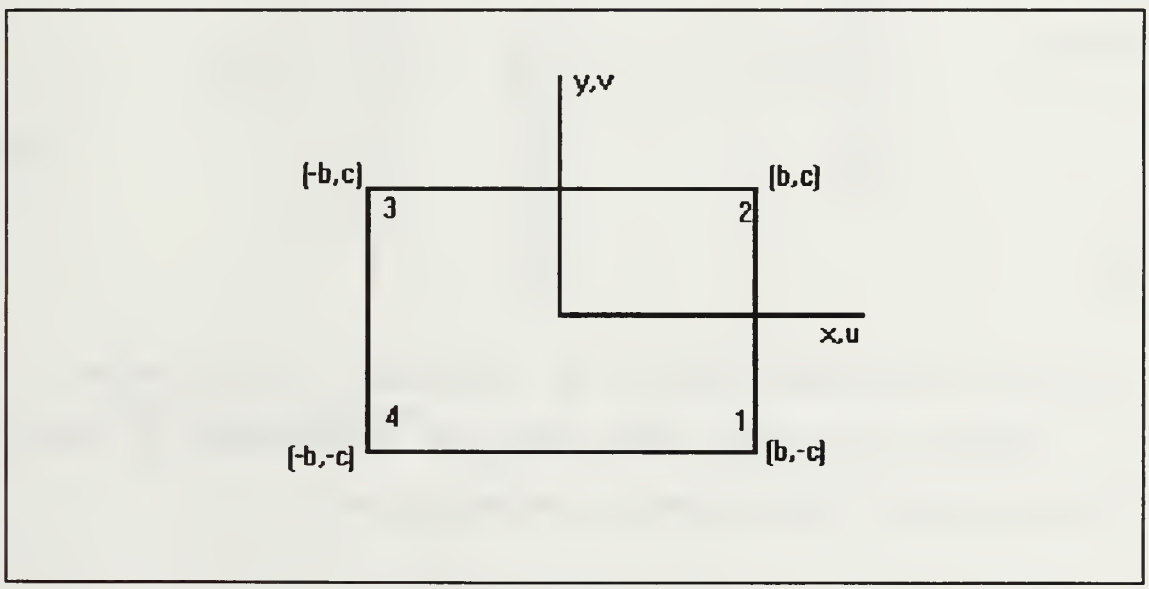

Figure 1 Bilinear Rectangular Element

The shape functions are

$$
\begin{aligned}
H_1 &= \frac{1}{4bc}(b-x)(c-y) \\
H_2 &= \frac{1}{4bc}(b+x)(c-y) \\
H_3 &= \frac{1}{4bc}(b+x)(c+y) \\
H_4 &= \frac{1}{4bc}(b-x)(c+y)
\end{aligned}
\tag{16}
$$

where b and c are greater than zero. The displacements in the x and y directions, respectively are interpolated as shown below

$$
\begin{aligned}
u &= H_1 u_1 + H_2 u_2 + H_3 u_3 + H_4 u_4 \\
v &= H_1 v_1 + H_2 v_2 + H_3 v_3 + H_4 v_4
\end{aligned}
\tag{17}
$$

where

$$
\begin{Bmatrix} u_1 \\ v_1 \\ u_2 \\ v_2 \\ u_3 \\ v_3 \\ u_4 \\ v_4 \end{Bmatrix}
\tag{18}
$$

is the displacement vector at the nodes of the element.

Because the shape functions are independent of time the acceleration terms become as shown below:

$$\begin{Bmatrix} \frac{\partial^2 u}{\partial t^2} \\ \frac{\partial^2 v}{\partial t^2} \end{Bmatrix} = \begin{Bmatrix} H_1 \ddot{u}_1 + H_2 \ddot{u}_2 + H_3 \ddot{u}_3 + H_4 \ddot{u}_4 \\ H_1 \ddot{v}_1 + H_2 \ddot{v}_2 + H_3 \ddot{v}_3 + H_4 \ddot{v}_4 \end{Bmatrix}$$

$$= \begin{bmatrix} H_1 & 0 & H_2 & 0 & H_3 & 0 & H_4 & 0 \\ 0 & H_1 & 0 & H_2 & 0 & H_3 & 0 & H_4 \end{bmatrix} \begin{Bmatrix} \ddot{u}_1 \\ \ddot{v}_1 \\ \ddot{u}_2 \\ \ddot{v}_2 \\ \ddot{u}_3 \\ \ddot{v}_3 \\ \ddot{u}_4 \\ \ddot{v}_4 \end{Bmatrix} . \qquad (19)$$

Substituting Eq.(19) back into Eq.(15) and applying Galerkin's method results in

$$\int_{\Omega} \rho \begin{bmatrix} H_1 & 0 \\ 0 & H_1 \\ H_2 & 0 \\ 0 & H_2 \\ H_3 & 0 \\ 0 & H_3 \\ H_4 & 0 \\ 0 & H_4 \end{bmatrix} \begin{bmatrix} H_1 & 0 & H_2 & 0 & H_3 & 0 & H_4 & 0 \\ 0 & H_1 & 0 & H_2 & 0 & H_3 & 0 & H_4 \end{bmatrix} d\Omega \begin{Bmatrix} \ddot{u}_1 \\ \ddot{v}_1 \\ \ddot{u}_2 \\ \ddot{v}_2 \\ \ddot{u}_3 \\ \ddot{v}_3 \\ \ddot{u}_4 \\ \ddot{v}_4 \end{Bmatrix} . \qquad (20)$$

Finally Eq.(20) becomes

$$\int_{\Omega^e}\rho\begin{bmatrix} H_1^2 & 0 & H_1H_2 & 0 & H_1H_3 & 0 & H_1H_4 & 0 \\ 0 & H_1^2 & 0 & H_1H_2 & 0 & H_1H_3 & 0 & H_1H_4 \\ H_1H_2 & 0 & H_2^2 & 0 & H_2H_3 & 0 & H_2H_4 & 0 \\ 0 & H_1H_2 & 0 & H_2^2 & 0 & H_2H_3 & 0 & H_2H_4 \\ H_1H_3 & 0 & H_2H_3 & 0 & H_3^2 & 0 & H_3H_4 & 0 \\ 0 & H_1H_3 & 0 & H_2H_3 & 0 & H_3^2 & 0 & H_3H_4 \\ H_1H_4 & 0 & H_2H_4 & 0 & H_3H_4 & 0 & H_4^2 & 0 \\ 0 & H_1H_4 & 0 & H_2H_4 & 0 & H_3H_4 & 0 & H_4^2 \end{bmatrix} d\Omega \begin{Bmatrix} \ddot{U}_1 \\ \ddot{V}_1 \\ \ddot{U}_2 \\ \ddot{V}_2 \\ \ddot{U}_3 \\ \ddot{V}_3 \\ \ddot{U}_4 \\ \ddot{V}_4 \end{Bmatrix} . \qquad (21)$$

Carrying out the integrations gives symmetric consistent mass matrix as shown below:

$$[M_c] = \frac{\rho}{9} bct \begin{bmatrix} 4 & 0 & 2 & 0 & 1 & 0 & 2 & 0 \\ & 4 & 0 & 2 & 0 & 1 & 0 & 2 \\ & & 4 & 0 & 2 & 0 & 1 & 0 \\ & & & 4 & 0 & 2 & 0 & 1 \\ & & & & 4 & 0 & 2 & 0 \\ & & & & & 4 & 0 & 2 \\ & & & & & & 4 & 0 \\ & & & & & & & 4 \end{bmatrix} \qquad (22)$$

where t is the thickness of the element. Equation (22) is called the consistent mass matrix.

Another choice for the mass matrix is the lumped mass matrix. The lumped mass matrix is a diagonal matrix so that it reduces computation time and space needed for storage. The

lumped mass matrix is

$$[M_l] = \rho bct \begin{bmatrix} 1 & 0 & 0 & 0 & 0 & 0 & 0 & 0 \\ & 1 & 0 & 0 & 0 & 0 & 0 & 0 \\ & & 1 & 0 & 0 & 0 & 0 & 0 \\ & & & 1 & 0 & 0 & 0 & 0 \\ & & & & 1 & 0 & 0 & 0 \\ & & & & & 1 & 0 & 0 \\ & & & & & & 1 & 0 \\ & & & & & & & 1 \end{bmatrix} . \tag{23}$$

D. STIFFNESS MATRIX

The stiffness matrix is given by

$$\int_{\Omega^e} \begin{bmatrix} \frac{\partial \omega_1}{\partial x} & 0 & \frac{\partial \omega_1}{\partial y} \\ 0 & \frac{\partial \omega_2}{\partial y} & \frac{\partial \omega_2}{\partial x} \end{bmatrix} \begin{Bmatrix} \sigma_x \\ \sigma_y \\ \tau_{xy} \end{Bmatrix} d\Omega \ . \tag{24}$$

Substituting constitutive equations, Eq.(2), into Eq.(24) yields

$$\int_{\Omega^e} \begin{bmatrix} \frac{\partial \omega_1}{\partial x} & 0 & \frac{\partial \omega_1}{\partial y} \\ 0 & \frac{\partial \omega_2}{\partial y} & \frac{\partial \omega_2}{\partial x} \end{bmatrix} [D] \begin{Bmatrix} \epsilon_x \\ \epsilon_y \\ \gamma_{xy} \end{Bmatrix} d\Omega \ . \tag{25}$$

Using kinematic equations, Eq. (25) becomes

$$\int_{\Omega^e} \begin{bmatrix} \frac{\partial \omega_1}{\partial x} & 0 & \frac{\partial \omega_1}{\partial y} \\ 0 & \frac{\partial \omega_2}{\partial y} & \frac{\partial \omega_2}{\partial x} \end{bmatrix} [D] \begin{Bmatrix} \frac{\partial u}{\partial x} \\ \frac{\partial v}{\partial y} \\ \frac{\partial v}{\partial x} + \frac{\partial u}{\partial y} \end{Bmatrix} d\Omega \ . \qquad (26)$$

The kinematic equation can be written in terms of the nodal displacements as below:

$$\begin{Bmatrix} \frac{\partial u}{\partial x} \\ \frac{\partial v}{\partial y} \\ \frac{\partial v}{\partial x} + \frac{\partial u}{\partial y} \end{Bmatrix} = \begin{bmatrix} \frac{\partial}{\partial x} & 0 & \frac{\partial}{\partial y} \\ 0 & \frac{\partial}{\partial y} & \frac{\partial}{\partial x} \end{bmatrix} \begin{Bmatrix} u \\ v \end{Bmatrix}$$

$$= \begin{bmatrix} \frac{\partial}{\partial x} & 0 & \frac{\partial}{\partial y} \\ 0 & \frac{\partial}{\partial y} & \frac{\partial}{\partial x} \end{bmatrix} \begin{bmatrix} H_1 & 0 & H_2 & 0 & H_3 & 0 & H_4 & 0 \\ 0 & H_1 & 0 & H_2 & 0 & H_3 & 0 & H_4 \end{bmatrix} \begin{Bmatrix} u_1 \\ v_1 \\ u_2 \\ v_2 \\ u_3 \\ v_3 \\ u_4 \\ v_4 \end{Bmatrix} \qquad (27)$$

$$= \begin{bmatrix} \frac{\partial H_1}{\partial x} & 0 & \frac{\partial H_2}{\partial x} & 0 & \frac{\partial H_3}{\partial x} & 0 & \frac{\partial H_4}{\partial x} & 0 \\ 0 & \frac{\partial H_1}{\partial y} & 0 & \frac{\partial H_2}{\partial y} & 0 & \frac{\partial H_3}{\partial y} & 0 & \frac{\partial H_4}{\partial y} \\ \frac{\partial H_1}{\partial y} & \frac{\partial H_1}{\partial x} & \frac{\partial H_2}{\partial y} & \frac{\partial H_2}{\partial x} & \frac{\partial H_3}{\partial y} & \frac{\partial H_3}{\partial x} & \frac{\partial H_4}{\partial y} & \frac{\partial H_4}{\partial x} \end{bmatrix} \begin{Bmatrix} u_1 \\ v_1 \\ u_2 \\ v_2 \\ u_3 \\ v_3 \\ u_4 \\ v_4 \end{Bmatrix}$$

where the last matrix is called [B] matrix and the last vector called the displacement vector {u}. Substituting back Eq.(27) into Eq.(25) yields

$$\int_{\Omega^e} \begin{bmatrix} \frac{\partial \omega_1}{\partial x} & 0 & \frac{\partial \omega_1}{\partial y} \\ 0 & \frac{\partial \omega_2}{\partial y} & \frac{\partial \omega_2}{\partial x} \end{bmatrix} [D]\,[B]\, d\Omega\{u\} \ . \tag{28}$$

Using Galerkin's method the first matrix in Eq.(28) becomes

$$\begin{bmatrix} \frac{\partial \omega_1}{\partial x} & 0 & \frac{\partial \omega_1}{\partial y} \\ 0 & \frac{\partial \omega_2}{\partial y} & \frac{\partial \omega_2}{\partial x} \end{bmatrix} = \begin{bmatrix} \frac{\partial H_1}{\partial x} & 0 & \frac{\partial H_1}{\partial y} \\ 0 & \frac{\partial H_1}{\partial y} & \frac{\partial H_1}{\partial x} \\ \frac{\partial H_2}{\partial x} & 0 & \frac{\partial H_2}{\partial y} \\ 0 & \frac{\partial H_2}{\partial y} & \frac{\partial H_2}{\partial x} \\ \frac{\partial H_3}{\partial x} & 0 & \frac{\partial H_3}{\partial y} \\ 0 & \frac{\partial H_3}{\partial y} & \frac{\partial H_3}{\partial x} \\ \frac{\partial H_4}{\partial x} & 0 & \frac{\partial H_4}{\partial y} \\ 0 & \frac{\partial H_4}{\partial y} & \frac{\partial H_4}{\partial x} \end{bmatrix} \tag{29}$$

which is equal to the transpose of B matrix.

Finally, the stiffness matrix is

$$[K] = \int_{\Omega^e} [B]^T [D] [B] \, d\Omega . \tag{30}$$

Computing the [K] matrix using bilinear rectangular element gives

$$\int_{-c}^{c}\int_{-b}^{b} [B]^t [D] [B] \, t \, dx dy \tag{31}$$

where t is the thickness, and

$$[B] = \frac{1}{4bc}\begin{bmatrix} -(c-y) & 0 & (c-y) & 0 & (c+y) & 0 & -(c+y) & 0 \\ 0 & -(b-x) & 0 & -(b+x) & 0 & (b+x) & 0 & (b-x) \\ -(b-x) & -(c-y) & -(b+x) & (c-y) & (b+x) & (c+y) & (b-x) & (c+y) \end{bmatrix} \tag{32}$$

For a general material property matrix [D] of Eq.(6), the element stiffness matrix becomes

$$[K] = \begin{bmatrix} K_{11} & K_{12} & K_{13} & K_{14} & K_{15} & K_{16} & K_{17} & K_{18} \\ K_{21} & K_{22} & K_{23} & K_{24} & K_{25} & K_{26} & K_{27} & K_{28} \\ K_{31} & K_{32} & K_{33} & K_{34} & K_{35} & K_{36} & K_{37} & K_{38} \\ K_{41} & K_{42} & K_{43} & K_{44} & K_{45} & K_{46} & K_{47} & K_{48} \\ K_{51} & K_{52} & K_{53} & K_{54} & K_{55} & K_{56} & K_{57} & K_{58} \\ K_{61} & K_{62} & K_{63} & K_{64} & K_{65} & K_{66} & K_{67} & K_{68} \\ K_{71} & K_{72} & K_{73} & K_{74} & K_{75} & K_{76} & K_{77} & K_{78} \\ K_{81} & K_{82} & K_{83} & K_{84} & K_{85} & K_{86} & K_{87} & K_{88} \end{bmatrix} . \tag{33}$$

The detail of K_{ij} is shown in the Appendix.

If a material is isotropic and the plane strain condition applies, the stiffness matrix is

$$[K] = [K_n] + [K_s] \quad . \tag{34}$$

$[K_n]$ is given by

$$A\begin{bmatrix}
\frac{16}{3}b^3c & 4ab^2c^2 & \frac{8}{3}b^3c & -4ab^2c^2 & \frac{-8}{3}b^3c & -4ab^2c^2 & \frac{-16}{3}b^3c & 4ab^2c^2 \\
 & \frac{16}{3}bc^3 & 4ab^2c^2 & \frac{-16}{3}bc^3 & -4ab^2c^2 & \frac{-8}{3}bc^3 & -4ab^2c^2 & \frac{8}{3}bc^3 \\
 & & \frac{16}{3}b^3c & -4ab^2c^2 & \frac{-16}{3}b^3c & -4ab^2c^2 & \frac{-8}{3}b^3c & 4ab^2c^2 \\
 & & & \frac{16}{3}bc^3 & 4ab^2c^2 & \frac{8}{3}bc^3 & 4ab^2c^2 & \frac{-8}{3}bc^3 \\
 & & & & \frac{16}{3}b^3c & 4ab^2c^2 & \frac{8}{3}b^3c & -4ab^2c^2 \\
 & & & & & \frac{16}{3}bc^3 & 4ab^2c^2 & \frac{-16}{3}bc^3 \\
 & & & & & & \frac{16}{3}b^3c & -4ab^2c^2 \\
 & & & & & & & \frac{16}{3}bc^3
\end{bmatrix} \tag{35}$$

where

$$A = \frac{E(1-\upsilon)\,t}{(4bc)^2(1+\upsilon)(1-2\upsilon)}$$

$$a = \frac{\upsilon}{(1-\upsilon)} \tag{36}$$

and $[K_s]$ is given by

$$B\begin{bmatrix}
\frac{16}{3}b^3c & 4b^2c^2 & \frac{8}{3}b^3c & -4b^2c^2 & \frac{-8}{3}b^3c & -4b^2c^2 & \frac{-16}{3}b^3c & 4b^2c^2 \\
 & \frac{16}{3}bc^3 & 4b^2c^2 & \frac{-16}{3}bc^3 & -4b^2c^2 & \frac{-8}{3}bc^3 & -4b^2c^2 & \frac{8}{3}bc^3 \\
 & & \frac{16}{3}b^3c & -4b^2c^2 & \frac{-16}{3}b^3c & -4b^2c^2 & \frac{-8}{3}b^3c & 4b^2c^2 \\
 & & & \frac{16}{3}bc^3 & 4b^2c^2 & \frac{8}{3}bc^3 & 4b^2c^2 & \frac{-8}{3}bc^3 \\
 & & & & \frac{16}{3}b^3c & 4b^2c^2 & \frac{8}{3}b^3c & -4b^2c^2 \\
 & & & & & \frac{16}{3}bc^3 & 4b^2c^2 & \frac{-16}{3}bc^3 \\
 & & & & & & \frac{16}{3}b^3c & -4b^2c^2 \\
 & & & & & & & \frac{16}{3}bc^3
\end{bmatrix} \quad (37)$$

where

$$B=\frac{Et}{2(4bc)^2(1+\upsilon)} \quad . \quad (38)$$

E. LOAD VECTOR

The load vector is given by

$$\int_\Gamma \begin{Bmatrix} \Phi_x \omega_1 \\ \Phi_y \omega_2 \end{Bmatrix} d\Gamma \quad . \quad (39)$$

Linear shape functions can be used to find nodal load values due to the traction. This results in lumping tractions into

two nodal points associated with the boundary of the element. If there is no traction, the load vector is zero at the associated nodal points. Linear shape functions are

$$H_1 = \frac{s_{i+1} - s}{h_i}$$
$$H_2 = \frac{s - s_i}{h_i} \qquad (40)$$
$$h_i = s_{i+1} - s_i$$

where s is the coordinate axis along the boundary, and h_i is the length of the boundary of the element. Combining all of the above procedure gives an equation of matrix,

$$[M]\{\ddot{u}\} + [K]\{u\} = \{R\} \qquad (41)$$

which describes the equation of motion with no damping. Damping was neglected in Eq.(41).

F. LINEAR TRIANGULAR ELEMENT

Since this study deals also with the linear triangular element, the derivation of the matrices will be shown here, but not in detail since the detail was shown before in the bilinear rectangular element case. The linear triangular element, as shown in Figure 2, has three nodal points which have coordinate values $(x_1,y_1),(x_2,y_2)$, and (x_3,y_3) respectively. Linear triangular element has two degrees of freedom per node.

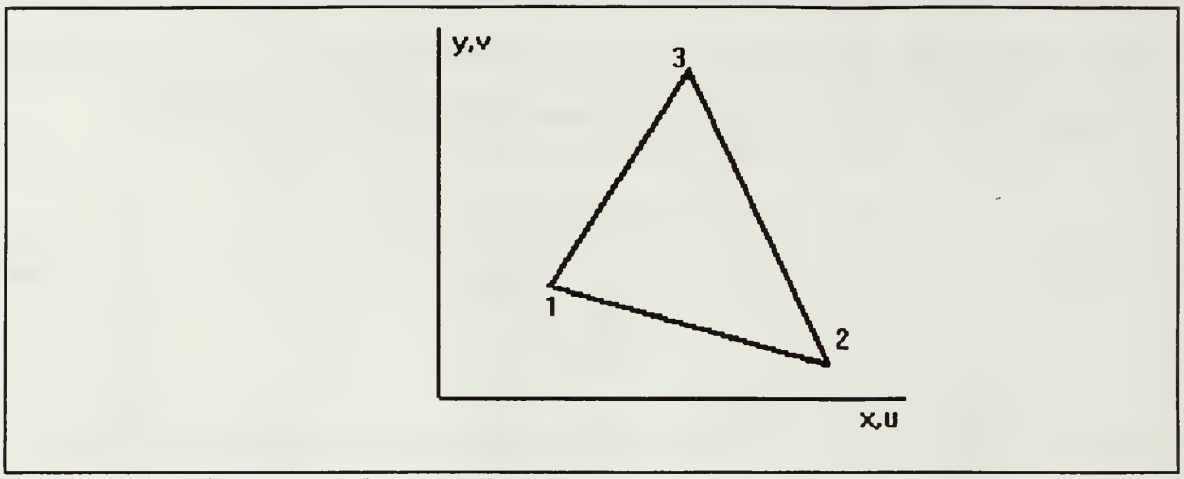

Figure 2 Linear triangular element

Note that three nodal points are numbered in the counter-clockwise direction from an arbitrarily selected corner.

The shape functions are

$$H_1=\frac{1}{2A}\left[A_1+B_1x+C_1y\right]$$
$$H_2=\frac{1}{2A}\left[A_2+B_2x+C_2y\right] \qquad (42)$$
$$H_3=\frac{1}{2A}\left[A_3+B_3x+C_3y\right]$$

where A is the area of the triangle, in other words

$$A=\frac{1}{2}\ \det\begin{bmatrix}1 & x_1 & y_1\\ 1 & x_2 & y_2\\ 1 & x_3 & y_3\end{bmatrix} \qquad (43)$$

and

$$
\begin{aligned}
A_1 &= x_2 y_3 - x_3 y_2 \qquad & B_1 &= y_2 - y_3 \qquad & C_1 &= x_3 - x_2 \\
A_2 &= x_3 y_1 - x_1 y_3 \qquad & B_2 &= y_3 - y_1 \qquad & C_2 &= x_1 - x_3 \\
A_3 &= x_1 y_2 - x_2 y_1 \qquad & B_3 &= y_1 - y_2 \qquad & C_3 &= x_2 - x_1 \ .
\end{aligned}
\tag{44}
$$

It can be noted that

$$
A = (A_1 + A_2 + A_3)/2 \ . \tag{45}
$$

The displacements in the x and y directions are given by

$$
\begin{aligned}
u &= H_1 u_1 + H_2 u_2 + H_3 u_3 \\
v &= H_1 v_1 + H_2 v_2 + H_3 v_3 \ .
\end{aligned}
\tag{46}
$$

Carrying out similar calculations and procedure gives the symmetric consistent, and lumped mass matrices, respectively

$$
[M_c] = \frac{\rho}{4} A t \begin{bmatrix}
2 & 0 & 1 & 0 & 1 & 0 \\
 & 2 & 0 & 1 & 0 & 1 \\
 & & 2 & 0 & 1 & 0 \\
 & & & 2 & 0 & 1 \\
 & & & & 2 & 0 \\
 & & & & & 2
\end{bmatrix}
\tag{47}
$$

$$
[M_l] = \frac{\rho}{3} A t \begin{bmatrix}
1 & 0 & 0 & 0 & 0 & 0 \\
 & 1 & 0 & 0 & 0 & 0 \\
 & & 1 & 0 & 0 & 0 \\
 & & & 1 & 0 & 0 \\
 & & & & 1 & 0 \\
 & & & & & 1
\end{bmatrix} .
\tag{48}
$$

The stiffness matrix is obtained from a combination of two components

$$[K_n] = \frac{EV}{4A^2(1-\upsilon^2)} \begin{bmatrix} B_1^2 & B_1C_1\upsilon & B_1B_2 & B_1C_2\upsilon & B_1B_3 & B_1C_3\upsilon \\ & C_1^2 & C_1B_2\upsilon & C_1C_2 & C_1B_3\upsilon & C_1C_3 \\ & & B_2^2 & B_2C_2\upsilon & B_2B_3 & B_2C_3\upsilon \\ & & & C_2^2 & C_2B_3\upsilon & C_2C_3 \\ & & & & B_3^2 & B_3C_3\upsilon \\ & & & & & C_3^2 \end{bmatrix} \quad (49)$$

and

$$[K_S] = \frac{EV}{8A^2(1+\upsilon)} \begin{bmatrix} C_1^2 & C_1B_1 & C_1C_2 & C_1B_2 & C_1C_3 & C_1B_3 \\ & B_1^2 & B_1C_2 & B_1B_2 & B_1C_3 & B_1B_3 \\ & & C_2^2 & C_2B_2 & C_2C_3 & C_2B_3 \\ & & & B_2^2 & B_2C_3 & B_2B_3 \\ & & & & C_3^2 & C_3B_3 \\ & & & & & B_3^2 \end{bmatrix} \quad (50)$$

where V is the volume of the element, that is,

$$V = At \quad (51)$$

and t is the thickness of the element.

G. TRANSIENT ANALYSIS

In this study the central difference method is used as a time integration scheme. The equation of motion at time t is

$$[M]\{\ddot{u}\}^t+[C]\{\dot{u}\}^t+[K]\{u\}^t=\{R\}^t \quad . \tag{52}$$

The acceleration at time t is given by

$$\{\ddot{u}\}^t=\frac{1}{\Delta t^2}[\{u\}^{t-\Delta t}-2\{u\}^t+\{u\}^{t+\Delta t}] \quad . \tag{53}$$

The velocity at time t is

$$\{\dot{u}\}^t=\frac{1}{2\Delta t}[-\{u\}^{t-\Delta t}+\{u\}^{t+\Delta t}] \quad . \tag{54}$$

The error associated with the acceleration and velocity calculations are of order (Δt^2). Substituting the relations for acceleration and velocity into the equation of motion,

$$\begin{aligned}&(\frac{1}{(\Delta t)^2}[M]+\frac{1}{2\Delta t}[C])\{u\}^{t+\Delta t}=\\ &\{R\}^t-([K]-\frac{2}{(\Delta t)^2}[M])\{u\}^t-(\frac{1}{(\Delta t)^2}[M]-\frac{1}{2\Delta t}[C])\{u\}^{t-\Delta t} \quad .\end{aligned} \tag{55}$$

The method requires the solution at time $-\Delta t$. Using the equations of acceleration and velocity, letting time to be equal to zero and eliminating $\{u\}^{\Delta t}$ yield

$$\{u\}^{-\Delta t}=\{u\}^0-\Delta t\{\dot{u}\}^0+\frac{(\Delta t)^2}{2}\{\ddot{u}\}^0 \quad . \tag{56}$$

Note that $\{\ddot{u}\}^0$ can be found using the equation of motion, Eq. (52), at time zero since $\{\dot{u}\}^0$ and $\{u\}^0$ are known.

The central difference scheme is conditionally stable and requires that the time step Δt should be smaller than a

critical time step Δt_{cr}. The critical time step is given by

$$\Delta t_{cr} = \frac{T_{min}}{\pi} \tag{57}$$

where T_{min} is the smallest period.

Therefore the method can be summarized as;

1.Compute mass, damping, and stiffness matrices.

2.Compute $\{\ddot{u}\}^0$ from

$$[M]\{\ddot{u}\}^0 = \{R\}^0 - [C]\{\dot{u}\}^0 + [K]\{u\}^0 \tag{58}$$

where $\{u\}^0$,and $\{\dot{u}\}^0$ are initial conditions.

3.Compute

$$\{u\}^{-\Delta t} = \{u\}^0 - \Delta t\{\dot{u}\}^0 + \frac{(\Delta t)^2}{2}\{\ddot{u}\}^0 \ . \tag{59}$$

4.Compute effective mass matrix from,

$$[\hat{M}] = \frac{1}{(\Delta t)^2}[M] + \frac{1}{2\Delta t}[C] \ . \tag{60}$$

5.Compute the effective load vector at time t,

$$\{\hat{R}\}^t = \{R\}^t - \left([K] - \frac{2}{(\Delta t)^2}[M]\right)\{u\}^t - \left(\frac{1}{(\Delta t)^2}[M] - \frac{1}{2\Delta t}[C]\right)\{u\}^{t-\Delta t}. \tag{61}$$

6.Solve for displacements at time t+Δt from,

$$[\hat{M}]\{u\}^{t+\Delta t} = \{\hat{R}\}^t \ . \tag{62}$$

7.Compute accelerations and velocities at time t,

$$\{\ddot{u}\}^t=\frac{1}{\Delta t^2}[\{u\}^{t-\Delta t}-2\{u\}^t+\{u\}^{t+\Delta t}]$$
$$\{\dot{u}\}^t=\frac{1}{2\Delta t}[-\{u\}^{t-\Delta t}+\{u\}^{t+\Delta t}] \quad . \tag{63}$$

Note that steps 5-7 have to be performed repeatedly for each time increment.

H. DYNAMIC FRACTURE ANALYSIS

There are many parameters to describe the crack tip behavior for determination of the crack propagation and arrest. One of the parameters is the stress intensity factor, K, at a crack tip which is defined as

$$K=\lim_{r\to 0}\sqrt{2\pi r}\,\sigma_n(r,0,t) \tag{64}$$

where

$$\sigma_n=\sigma_n(r,\theta,t) \tag{65}$$

is the stress component, and is evaluated near the crack tip. In this case, crack propagation is governed by stress intensity factor K, and the material property K_c, called the fracture toughness. A crack becomes unstable if the stress intensity factor reaches the fracture toughness of the material.

The dynamic analysis requires K be considered in two parts. For crack initiation,

$$K(a,\sigma,t)=K_D(\dot{\sigma}) \tag{66}$$

where a is the crack length, σ is the applied stress, t is time, and $\dot{\sigma}$ represents the loading rate. For a propagating crack,

$$K(a,\sigma,t)=K_d(\dot{a}) \tag{67}$$

where $\dot{a}$ indicates the crack speed. [Ref. 7]

An alternative criterion for crack motion is,

$$G(a,\sigma,t)=R(\dot{a}) \tag{68}$$

where G is the dynamic energy release rate and R is the energy dissipation rate required for crack growth which is the critical value of G.

The driving force or the dynamic energy release rate for crack propagation has contributions from strain energy, kinetic energy, and work done on the body. The driving force is the net change in these components per unit area of crack extension. The equation for G is,

$$G=\frac{1}{b}\left(\frac{dW}{da}-\frac{dU}{da}-\frac{dT}{da}\right)$$
$$=\frac{1}{b\dot{a}}\left(\frac{dW}{dt}-\frac{dU}{dt}-\frac{dT}{dt}\right) \quad (69)$$

where U is the strain energy, T is the kinetic energy, W is the work done by the external loading, a is the crack length, and b is the plate thickness at the crack tip.

The dynamic energy release rate can be directly connected to the dynamic stress intensity factor. For plane strain conditions, this relation is

$$G=\frac{1-\upsilon^2}{E}A(\dot{a})K^2 \quad (70)$$

where E and υ, as usual, are the elastic modulus and Poisson's ratio, respectively, and A is a geometry independent function of the crack speed given by

$$A=\frac{\left(\frac{\dot{a}}{C_2}\right)^2\left(1-\frac{\dot{a}^2}{C_1^2}\right)^{\frac{1}{2}}}{(1-\upsilon)\left[4\left(1-\frac{\dot{a}^2}{C_1^2}\right)^{\frac{1}{2}}\left(1-\frac{\dot{a}^2}{C_2^2}\right)^{\frac{1}{2}}-\left(2-\frac{\dot{a}^2}{C_2^2}\right)^2\right]} \quad (71)$$

where C_1 and C_2, respectively, are longitudinal and shear (transverse) wave speeds in the material. Wave speeds are given by,

$$C_1=\left[\frac{(K_b+4G_s/3)}{\rho}\right]^{1/2} \quad (72)$$

and

$$C_2 = (G_s/\rho)^{1/2} \tag{73}$$

where K_b and G_s are bulk and shear modulus, respectively.

III. RESULTS AND DISCUSSION

A. VERIFICATION PROBLEMS

In order to verify the developed computer code, two example problems with known solutions were analyzed for isotropic plates. One was a stationary crack problem subjected to a rapidly varying dynamic load, and other was a propagating crack problem with a constant speed and subjected to a uniform load.

The first verification problem was a stationary crack problem known as Chen's problem [Ref.1]. A rectangular bar with a centrally located crack, shown in Figure 3, was considered. A uniform tension of magnitude 0.004 Mbar with Heaviside-function time dependence was applied. The material properties were given as below; shear modulus of 0.76923 Mbar, bulk modulus of 1.66667 Mbar, Poisson's ratio of 0.3, and material density of 5 gr/cm^3. Chen solved the problem using the finite difference technique.

Both Chen's solution and the present solution are shown in Figure 4. A good agreement between the two solutions was obtained.

As the second example a rectangular plate with a central, moving crack was considered [Ref. 3]. The crack was assumed to

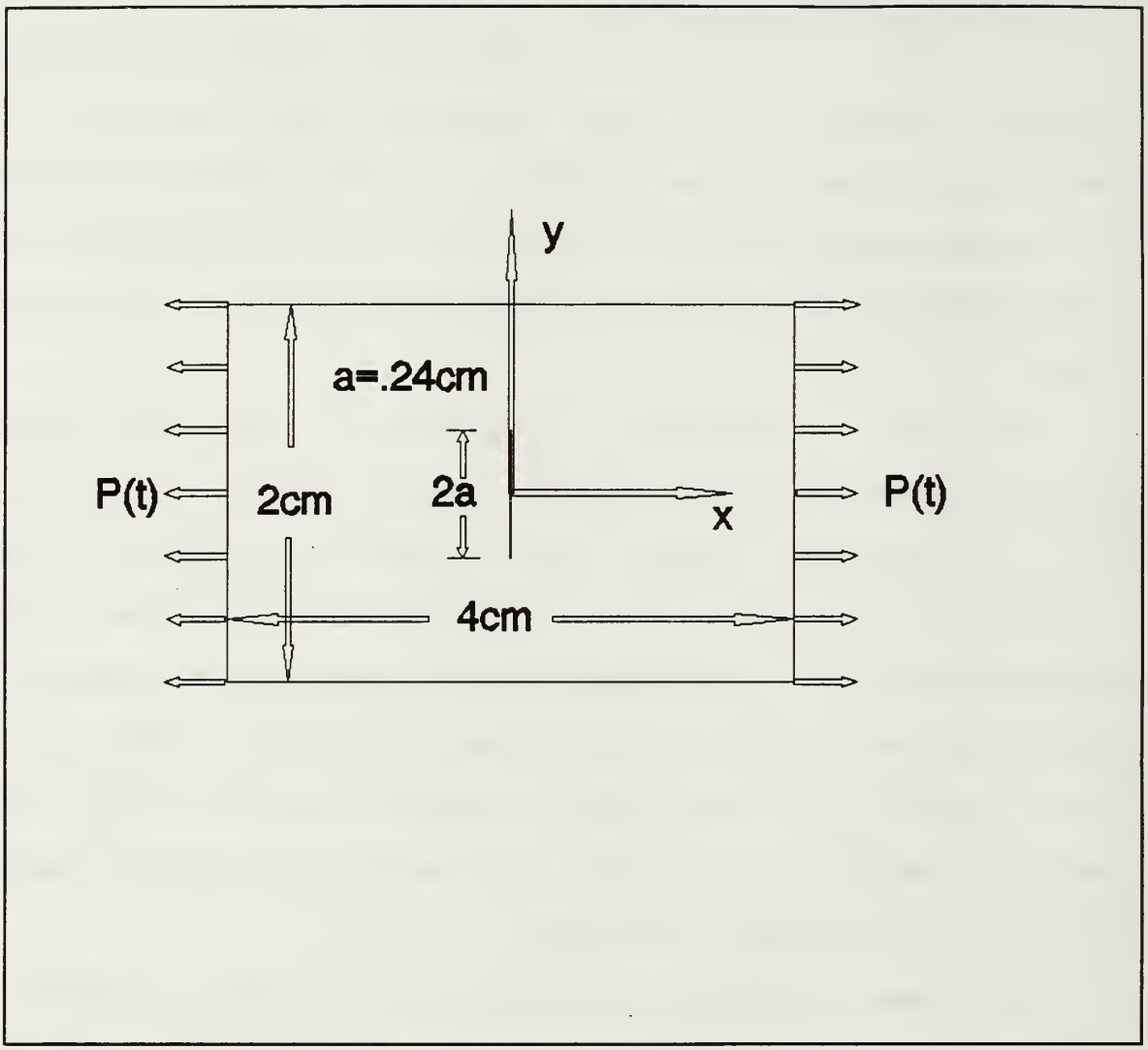

Figure 3 The Geometry of the Stationary Crack Problem

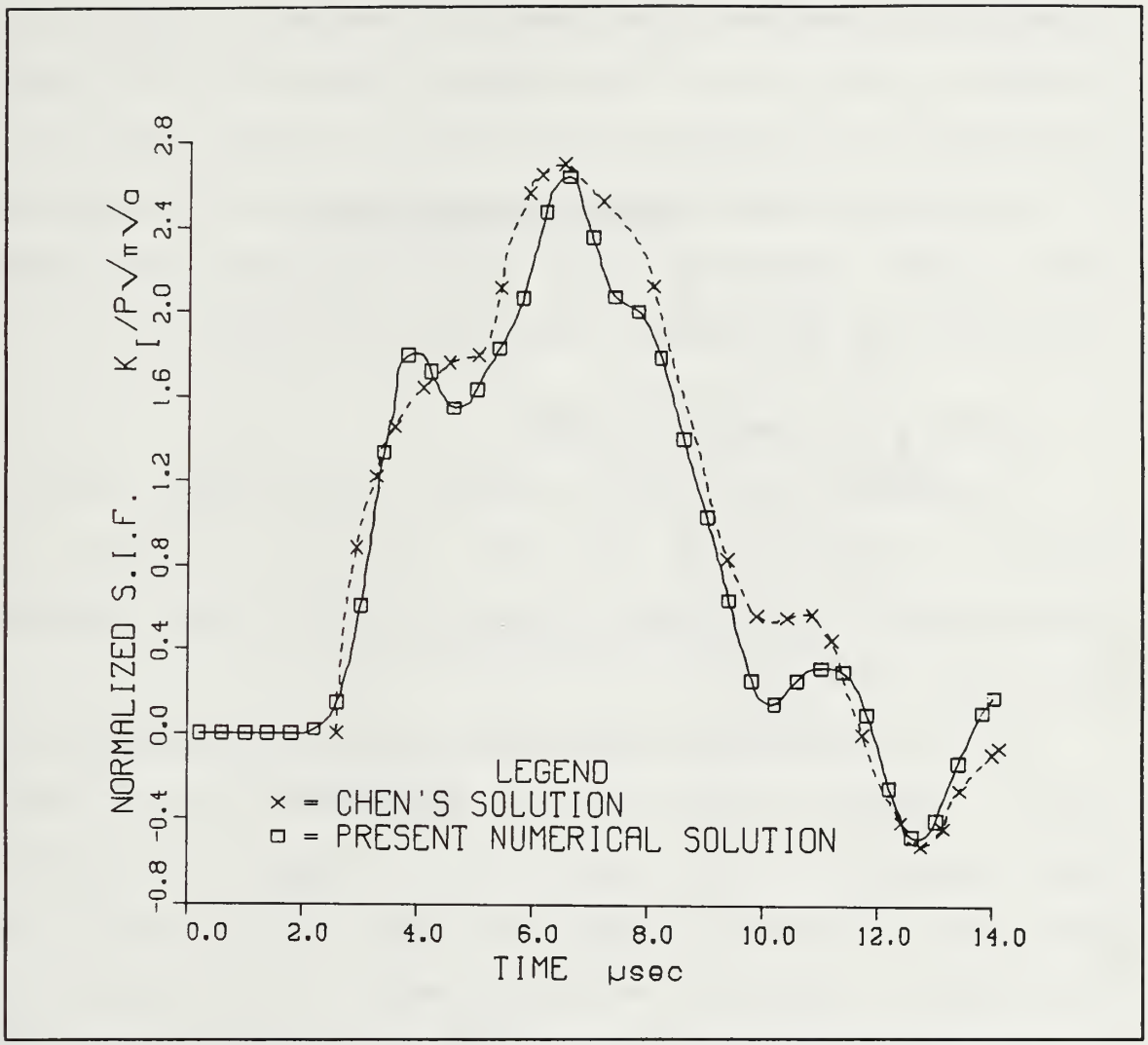

Figure 4 The Results of the Stationary Crack Problem

propagate at a constant speed with uniform stress field of 68.9 MPa. The crack speed was assumed to be 33% of the dilatational wave speed in a steel which is 5904 m/s. The material properties were elastic modulus of 206.7 GPa, Poisson's ratio of 0.30, and material density of 8000 kg/m^3. The geometry of the problem is shown in Figure 5.[Ref. 3]

A good agreement was obtained between the analytical and the present solutions. Both the analytical and present numerical analysis results are shown in Figure 6.

B. RESULTS OF COMPOSITE PLATES

A composite plate with a central, moving crack, with a similar configuration as the previous example, was investigated for different cases. A unidirectional composite plate was considered.

For all cases calculations were made for work done on the system, internal energy, kinetic energy and fracture energy. The objective of this study was to compare the fracture energies for various conditions. The first case was the variation of the ratio of elastic moduli of the longitudinal and the transverse directions while keeping the others fixed. The next case changed crack velocities and, the last case varied material densities while keeping the other parameters fixed. The geometric and material properties of the problem

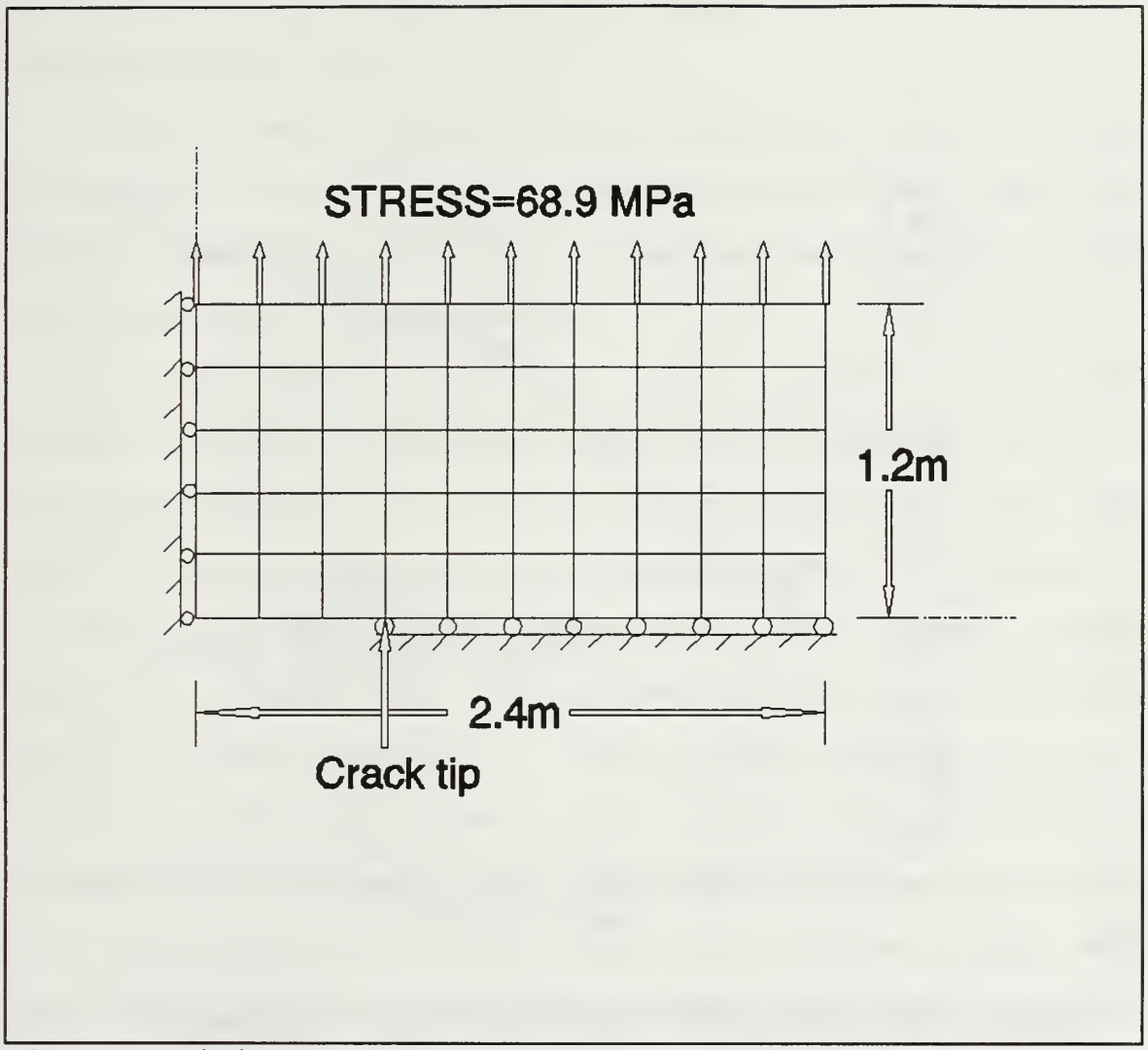

Figure 5 Finite Element Mesh for the Moving Crack Problem

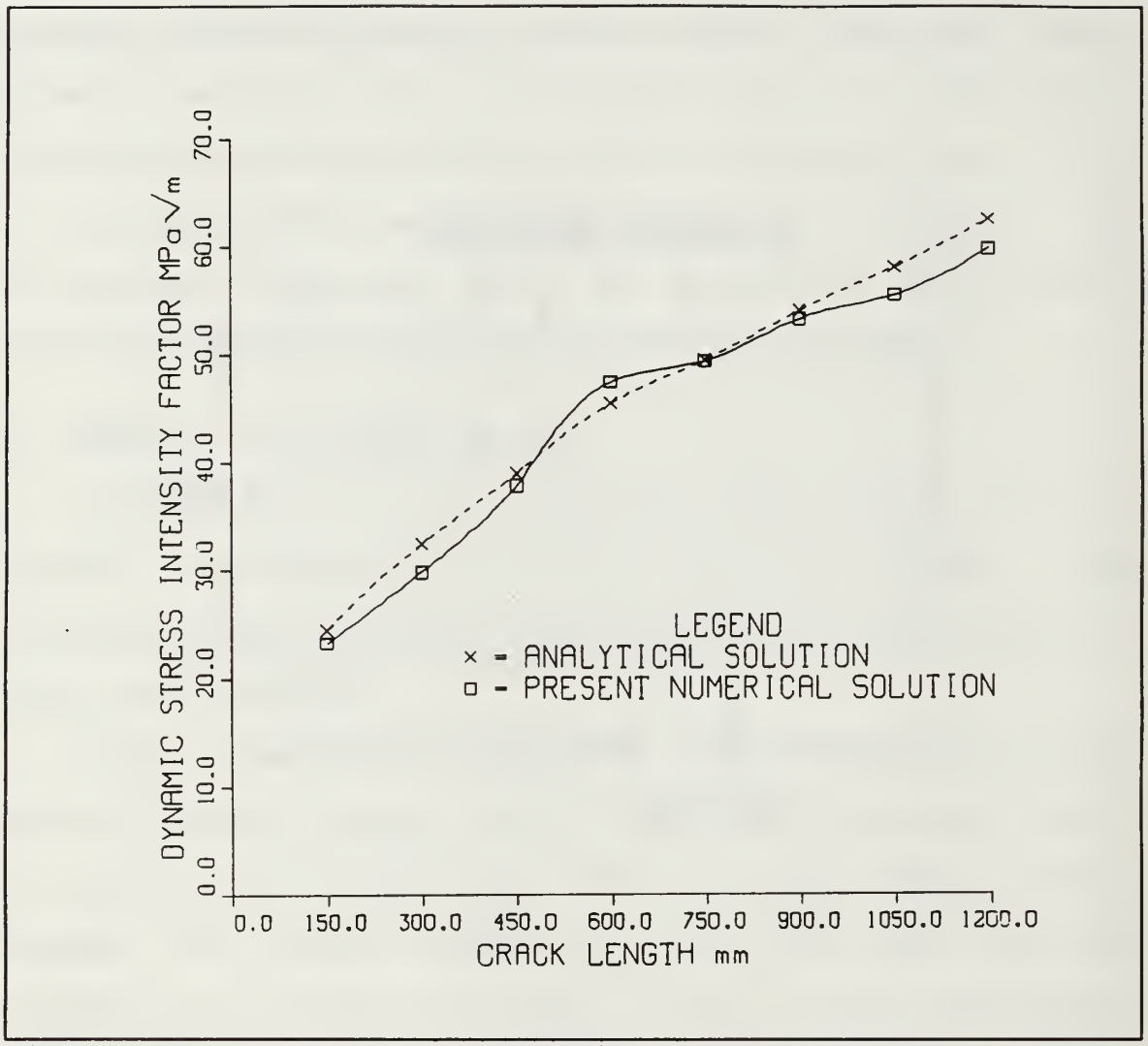

Figure 6 The Results of the Moving Crack Problem

are length of 3m, width of 1m, elastic modulus ratio in the transverse direction of 10 GPa, Poisson's ratio in the transverse direction associated with loading in longitudinal direction of 0.25, and uniform loading in the longitudinal direction of 70 MPa.

Figure 7 shows work and energy variations during a crack propagation. For all cases throughout this study, work was higher than internal and kinetic energies, and internal energy was higher than kinetic energy.

In the first case, the elastic modulus ratios were changed. Three different ratios between the elastic moduli in the longitudinal and transverse directions were used. The crack velocity and the material density were kept constant.

Figure 8 and Figure 9 show work and internal energy variation, respectively. The results reflect higher work and higher internal energy for a lower elastic modulus ratio. A softer material which has a lower elastic modulus ratio is subjected to a larger displacement under the same load while all other parameters held the same. This produces higher work and higher internal energy since they are proportional to displacements. As will be seen in all cases, the trends of work and internal energy are always similar to each other.

Figure 10 shows the kinetic energy variation. Kinetic energy is higher for a lower elastic modulus ratio, because

for this material the material velocity is higher due to the larger displacement. Figure 11 shows the fracture energy variation. Fracture energy is also higher for a lower elastic modulus ratio.

The increments of work and energies between the initial time and a later time are plotted in Figure 12. The larger fracture energy for a lower elastic modulus ratio was caused by a much larger increase of work relative to the increases of internal and kinetic energies for this material.

In the second case the crack velocity was varied. Three different crack velocities were used. The elastic modulus ratio and the material density were kept constant. Figure 13 and Figure 14 show work and internal energy variations, respectively. The time needed for a crack propagation to the same crack size increment is longer for a lower crack velocity. With a longer time, the crack propagation influences the rest of the body more widely. The wider influence results in a larger displacement. As a result, it produces higher work and higher internal energy. A typical displacement variation at a point, shown in Figure 15, clearly is larger for a lower crack velocity.

Figure 16 shows the kinetic energy variation. Kinetic energy is higher for a higher crack velocity. The reason is, as shown in Figure 17, a higher crack velocity produces higher

speeds in the material. Figure 18 shows the fracture energy variation. Fracture energy is higher for a lower crack velocity because a lower crack velocity caused a larger increase of work and a less increase of kinetic energy than a higher crack velocity.

The material density was varied as the last study. Three different material densities were used. The elastic modulus ratio and the crack velocity were kept constant. Figure 13 and Figure 14 show the work and internal energy variations, respectively. For the same magnitude of an external force, a smaller density causes a higher velocity and larger displacement of the plate. Because the displacement is larger for a lower material density, work and internal energy are higher. Figure 22 confirms it. Figure 23 also shows a higher speed for a lower material density.

Figure 24 shows the kinetic energy variation. Kinetic energy is higher for a higher material density. The velocity is higher for a lower density, but the mass is larger for a higher density. Because the kinetic energy is proportional to the mass as well as the square of velocity, which case gives a higher kinetic energy depends on which term is dominating. In this situation large mass yields a higher kinetic energy although the material velocity is lower. Figure 25 shows the fracture energy variation. Fracture energy is higher for a

lower material density because of the same reason as that for the case of different crack velocities. The increments of work and energies are also plotted in Figure 26.

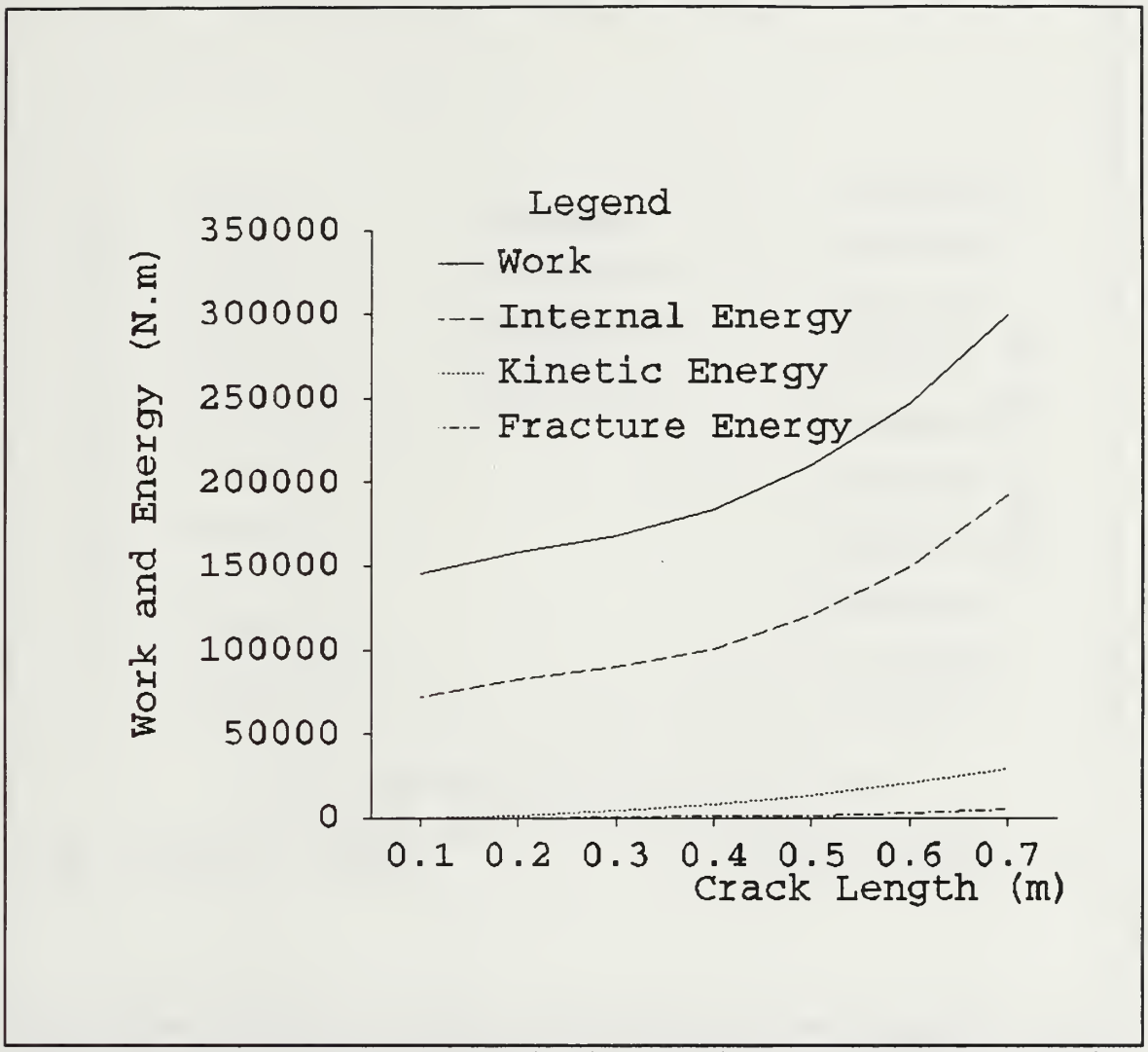

Figure 7 Work and Energy Variation During a Crack Propagation

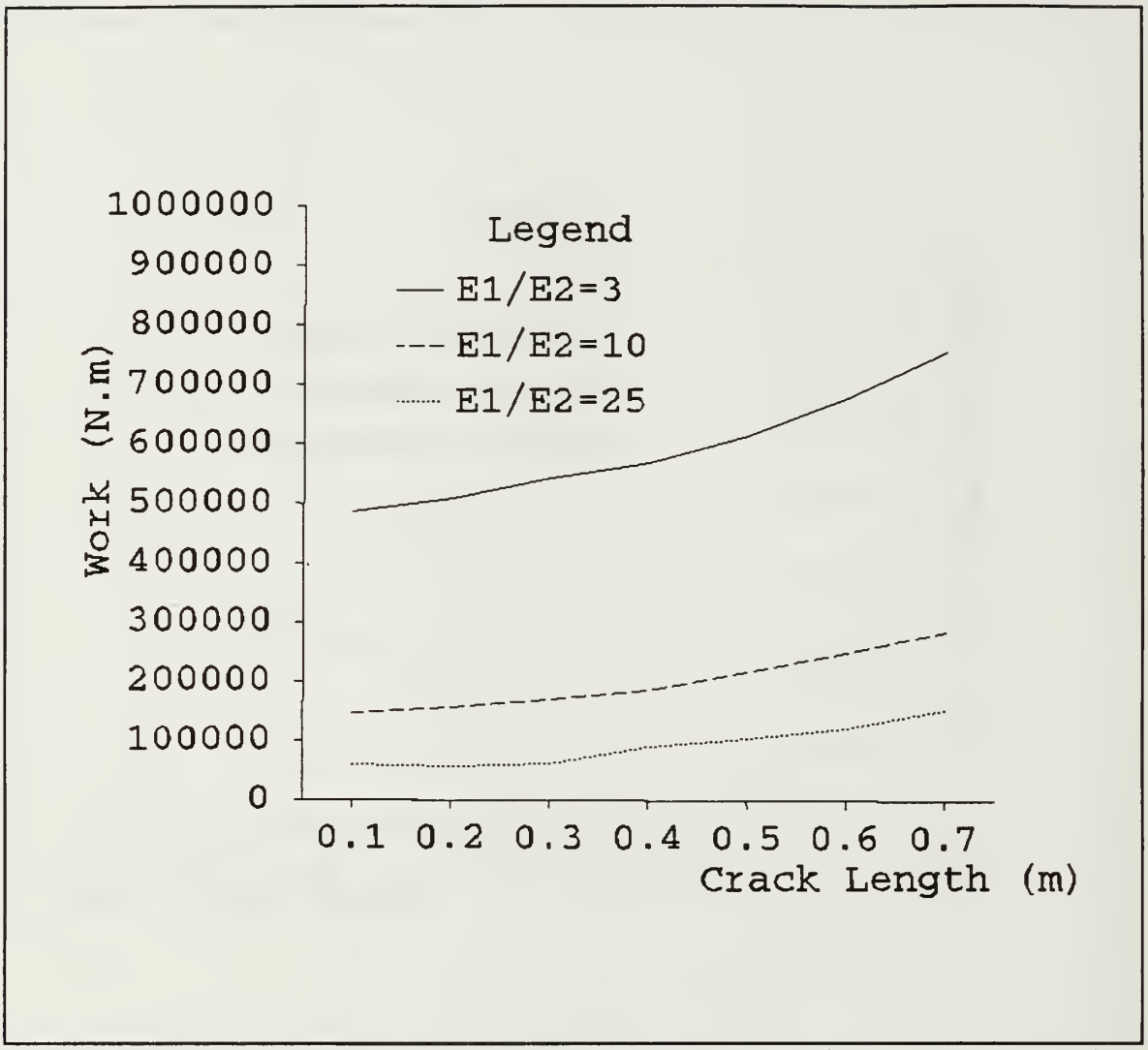

Figure 8 Work Variation for Different Elastic Modulus Ratios and Fixed Crack Velocity and Material Density

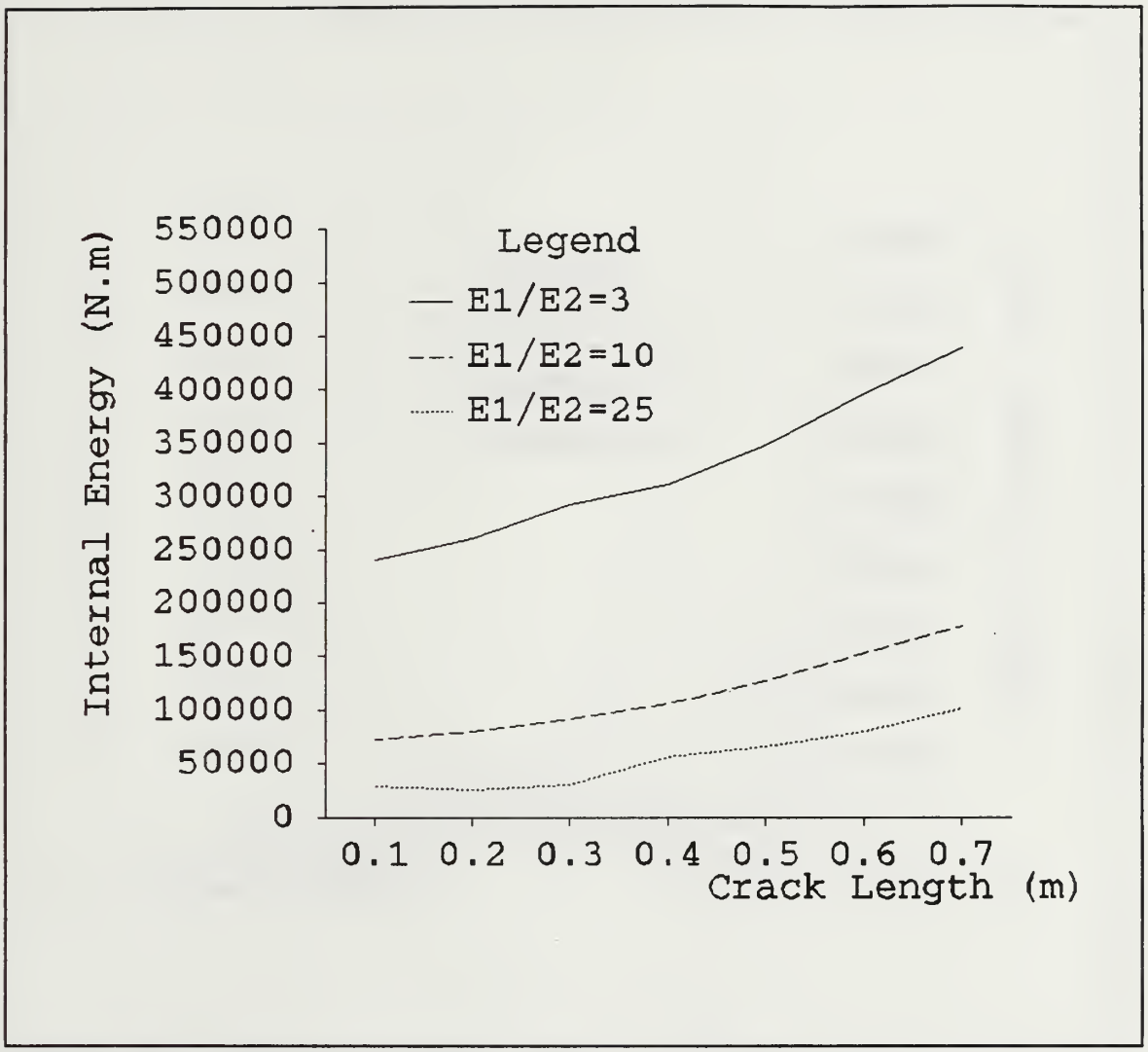

Figure 9 Internal Energy Variation for Different Elastic Modulus Ratios and Fixed Crack Velocity and Material Density

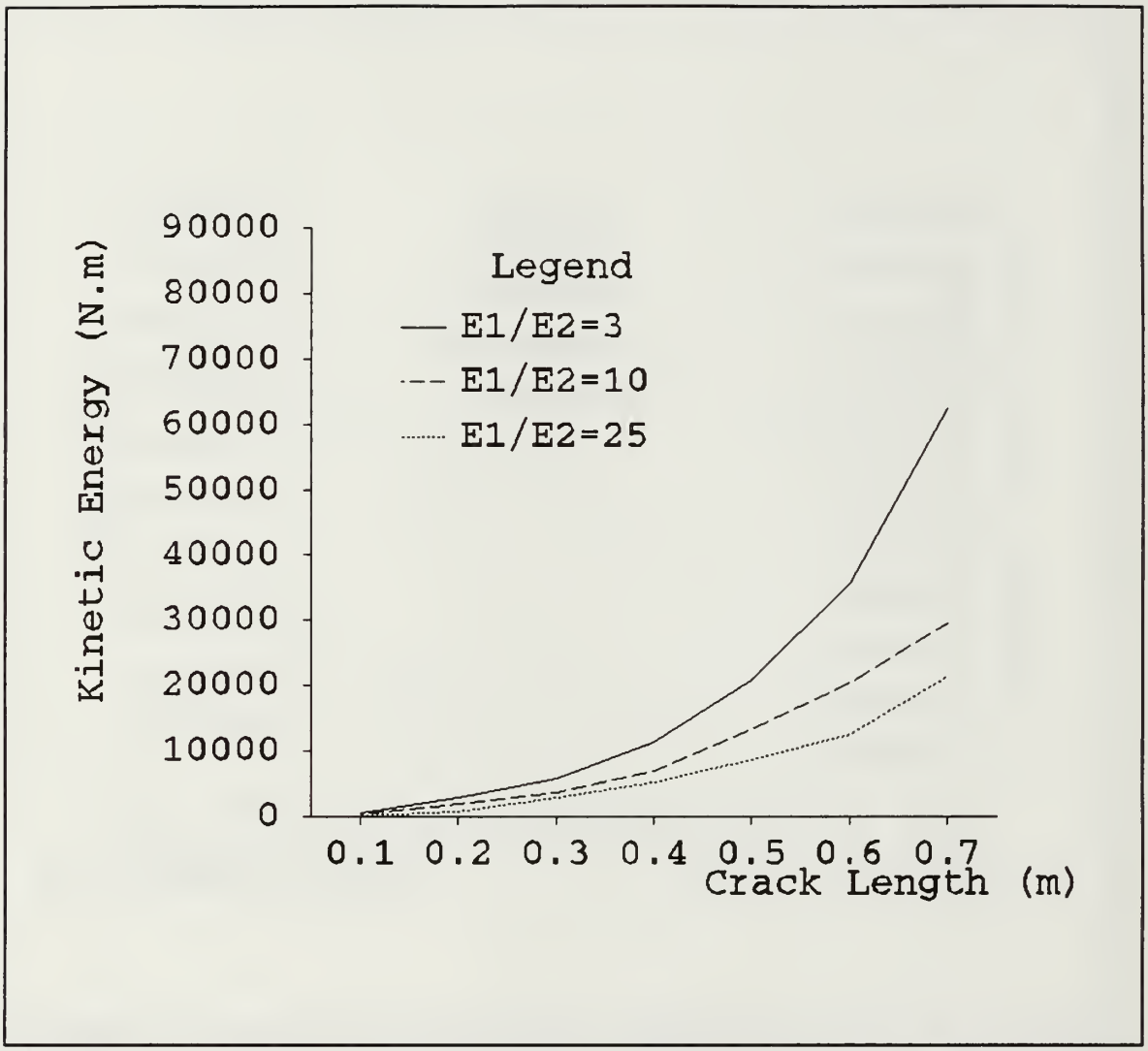

Figure 10 Kinetic Energy Variation for Different Elastic Modulus Ratios and Fixed Crack Velocity and Material Density

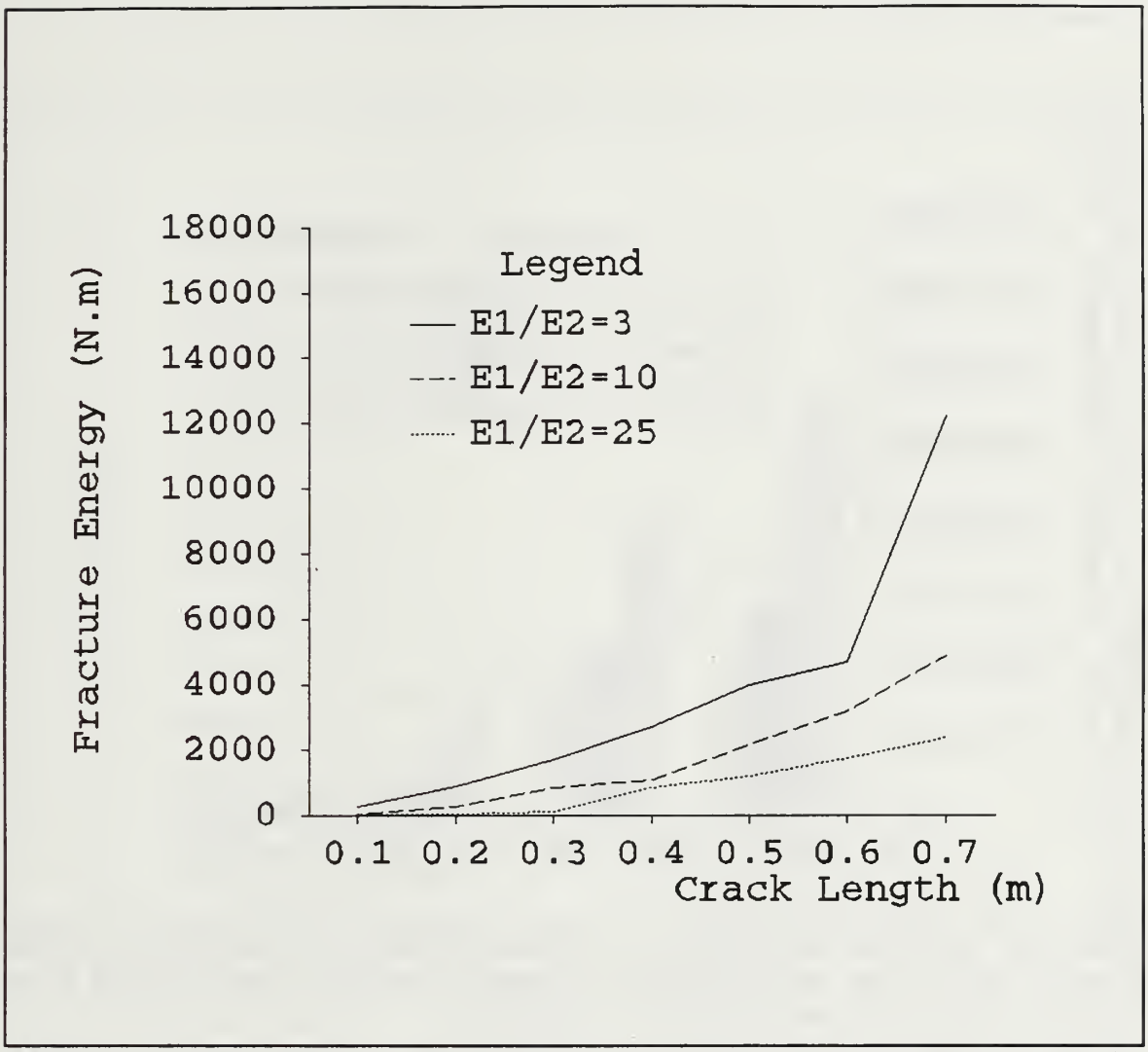

Figure 11 Fracture Energy Variation for Different Elastic Modulus Ratios and Fixed Crack Velocity and Material Density

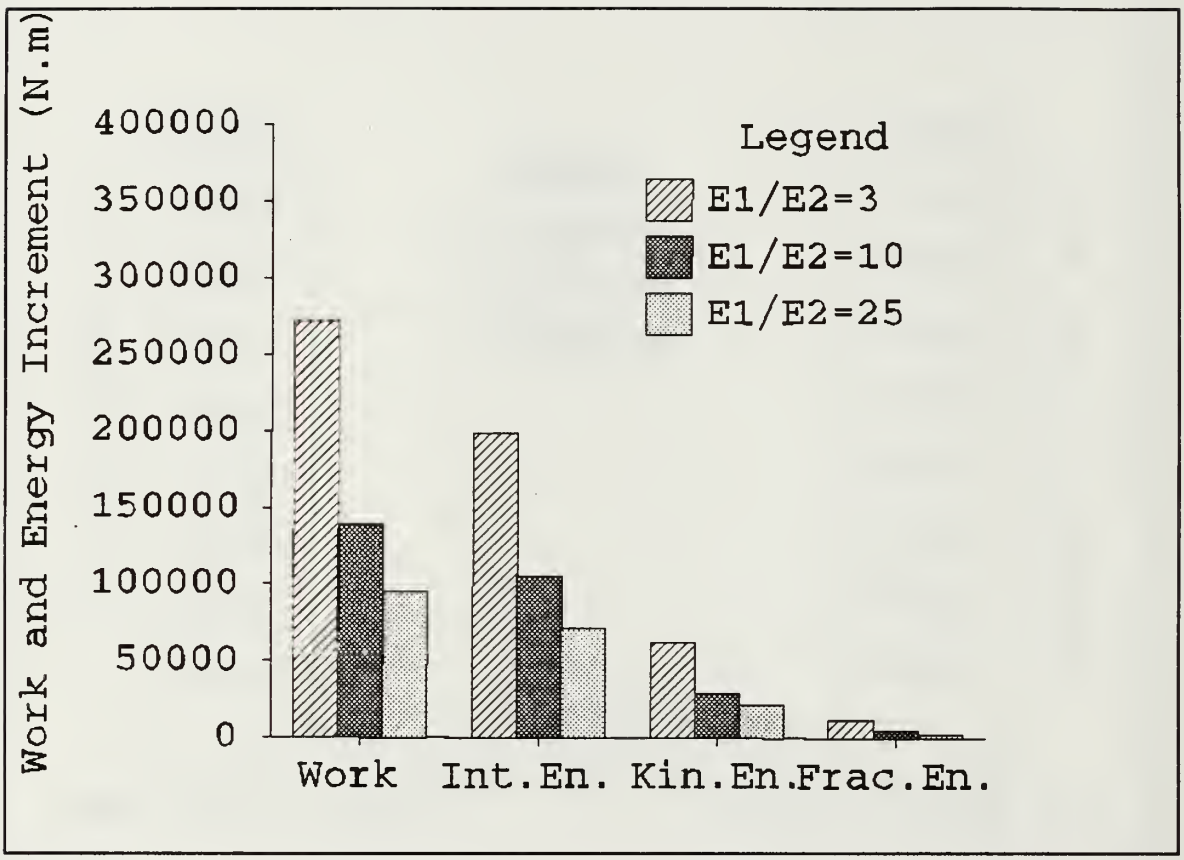

Figure 12 Work and Energy Differences Between the Initial Time and a Late Time for Different Elastic Modulus Ratios and Fixed Crack Velocity and Material Density

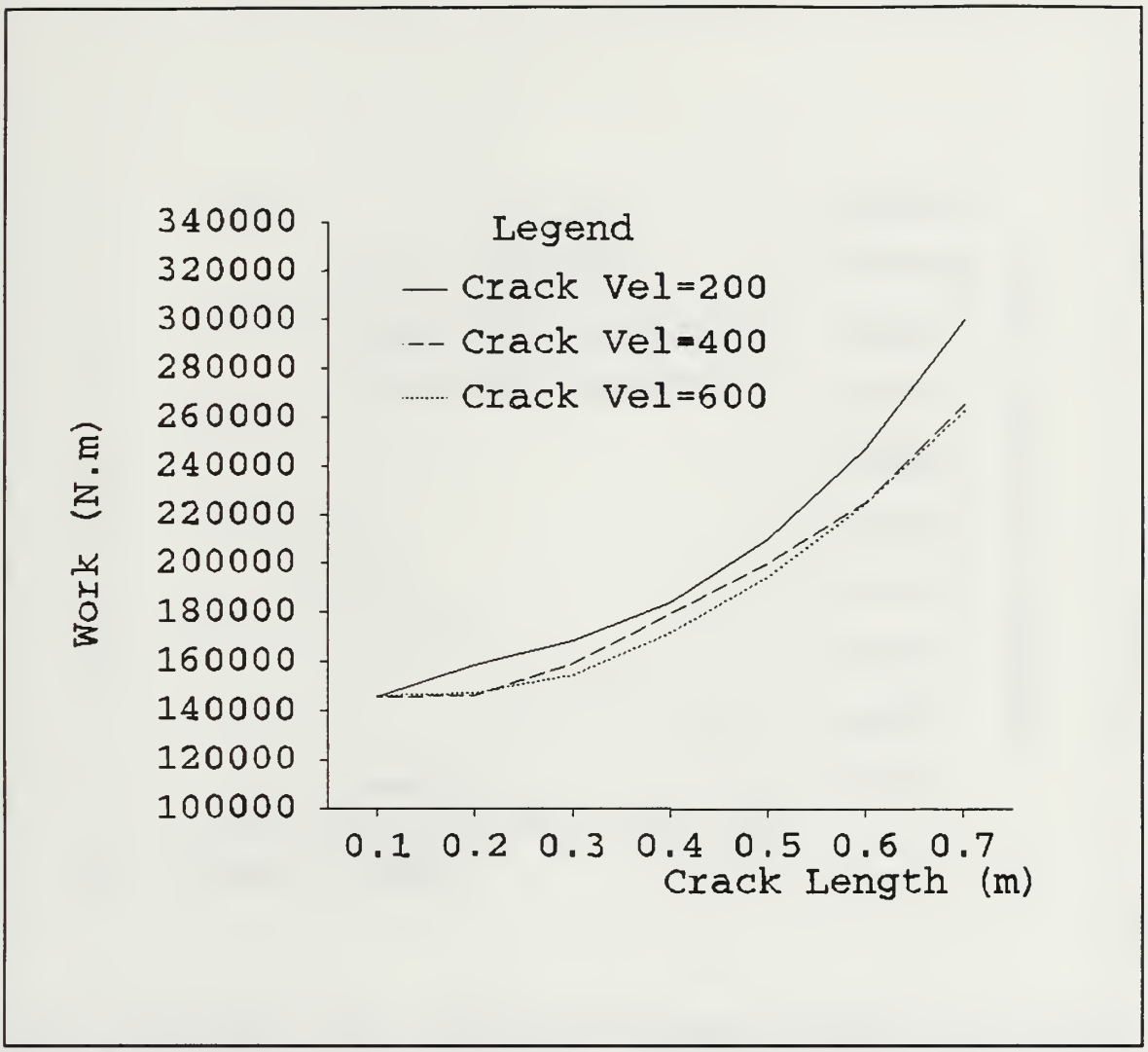

Figure 13 Work Variation for Different Crack Velocities and Fixed Elastic Modulus Ratio and Material Density

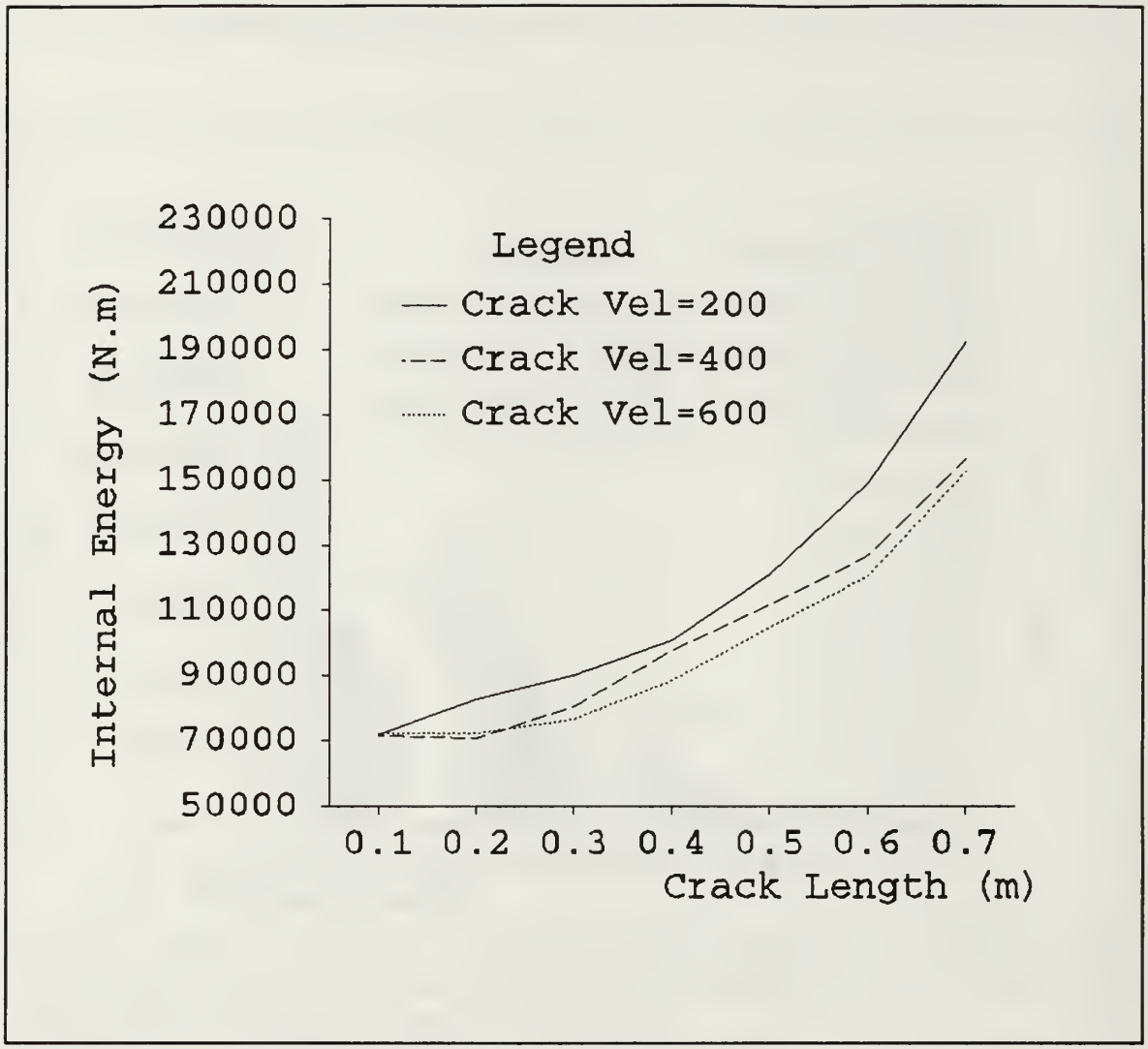

Figure 14 Internal Energy Variation for Different Crack Velocities and Fixed Elastic Modulus Ratio and Material Density

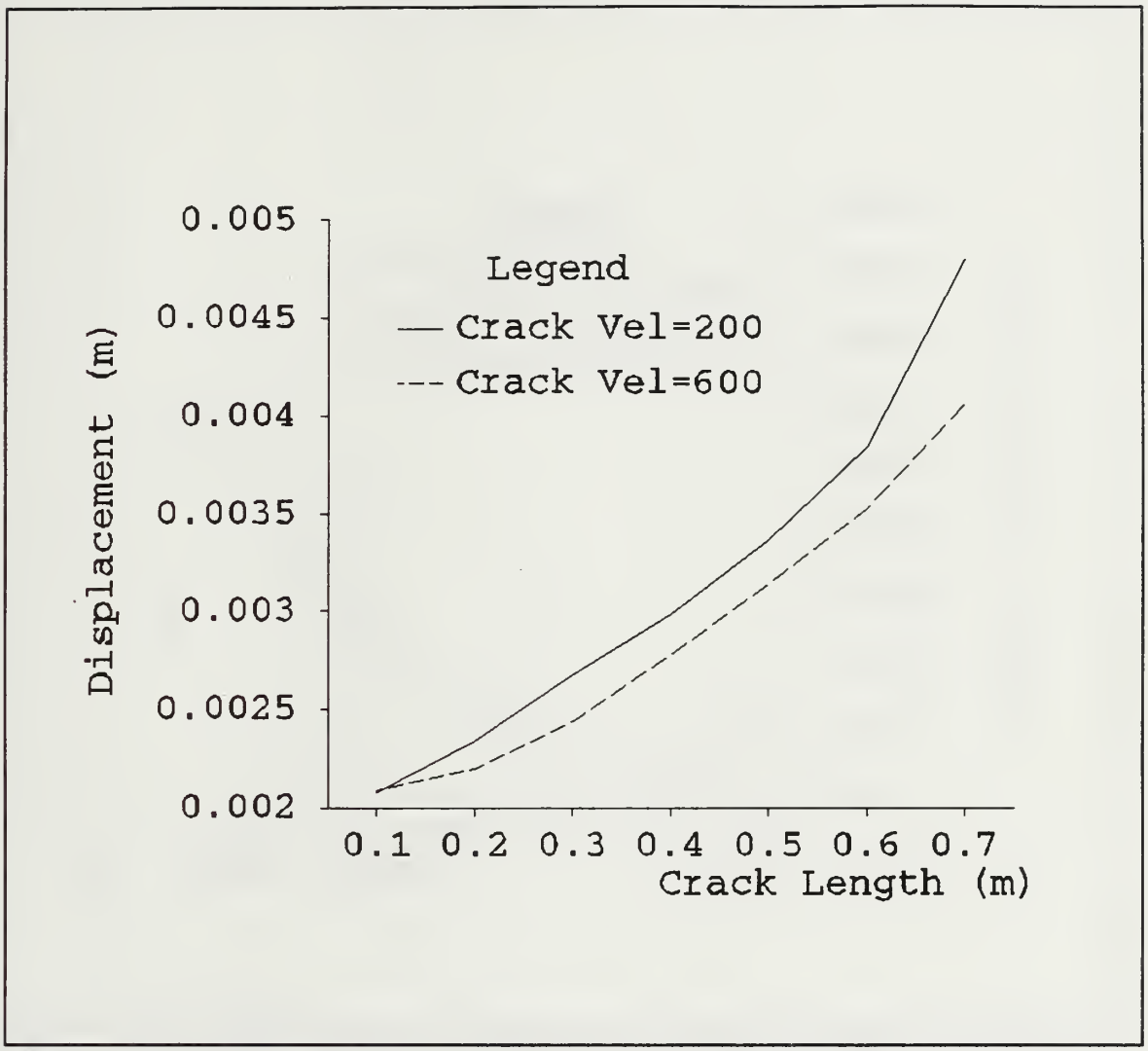

Figure 15 Displacement Values for Different Crack Velocities and Fixed Elastic Modulus Ratio and Material Density

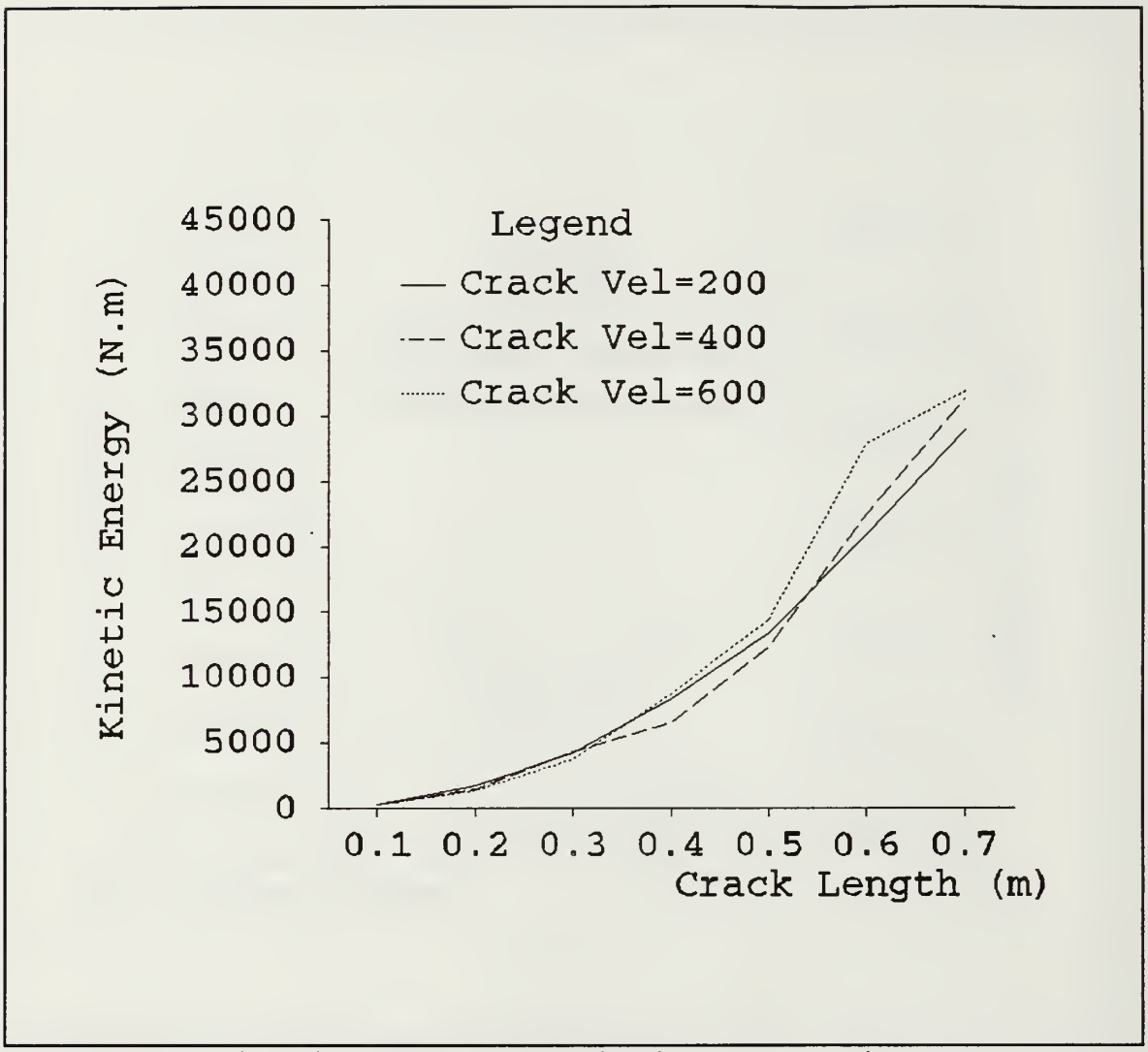

Figure 16 Kinetic Energy Variation for Different Crack Velocities and Fixed Elastic Modulus Ratio and Material Density

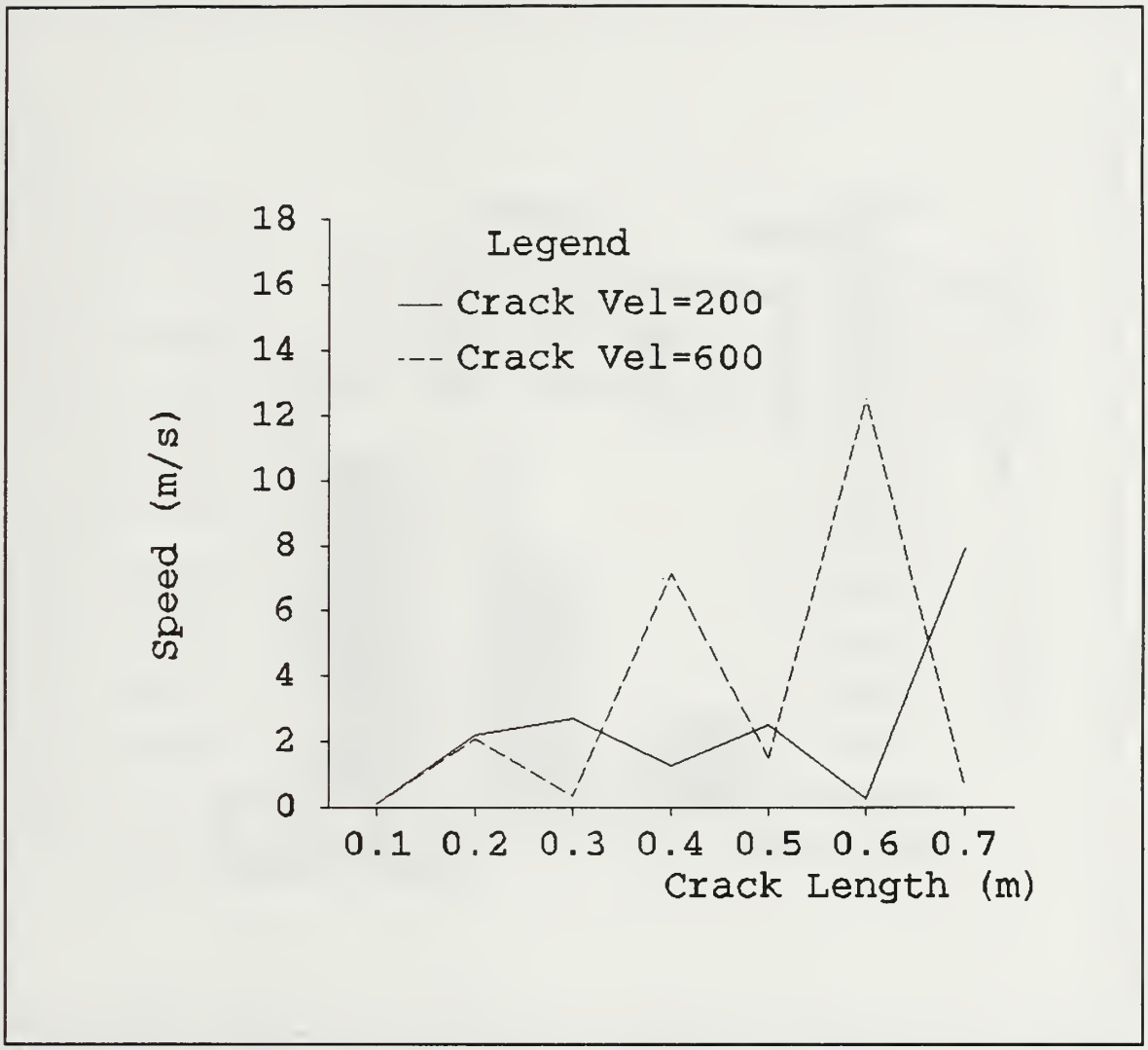

Figure 17 Speed Values for Different Crack Velocities and Fixed Elastic Modulus Ratio and Material Density

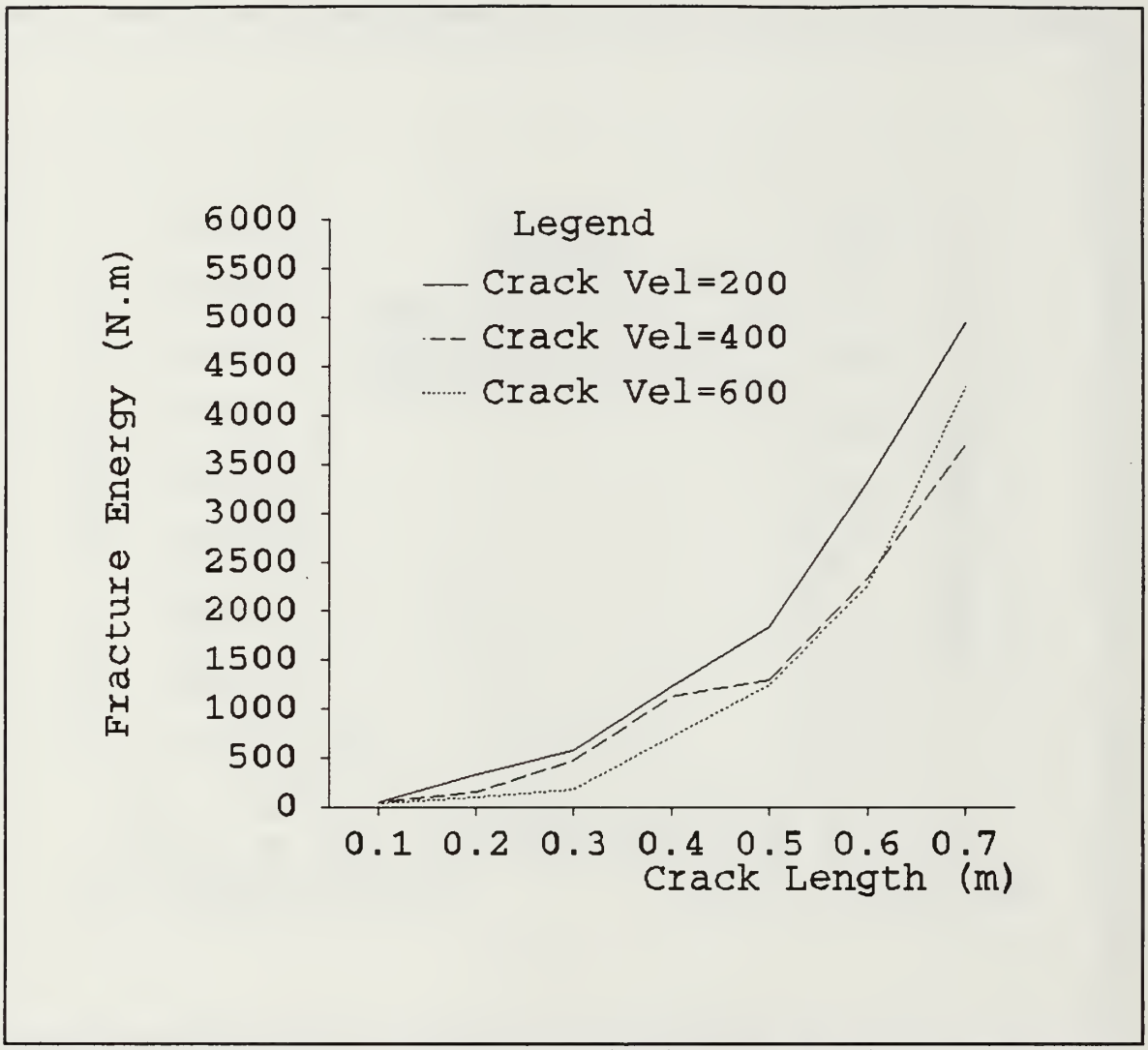

Figure 18 Fracture Energy Variation for Different Crack Velocities and Fixed Elastic Modulus Ratio and Material Density

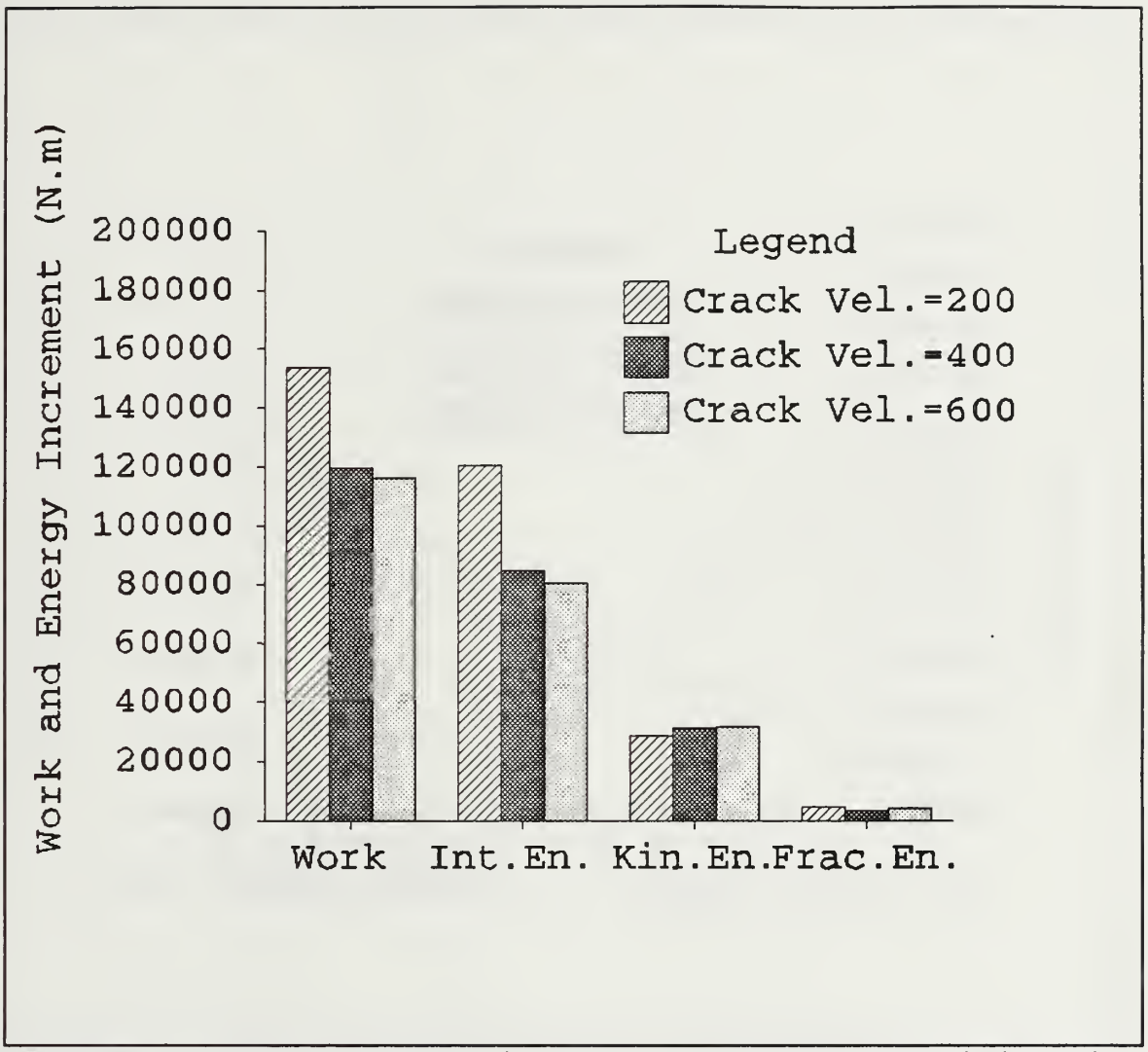

Figure 19 Work and Energy Differences Between the Initial Time and a Late Time for Different Crack Velocities and Fixed Elastic Modulus Ratio and Material Density

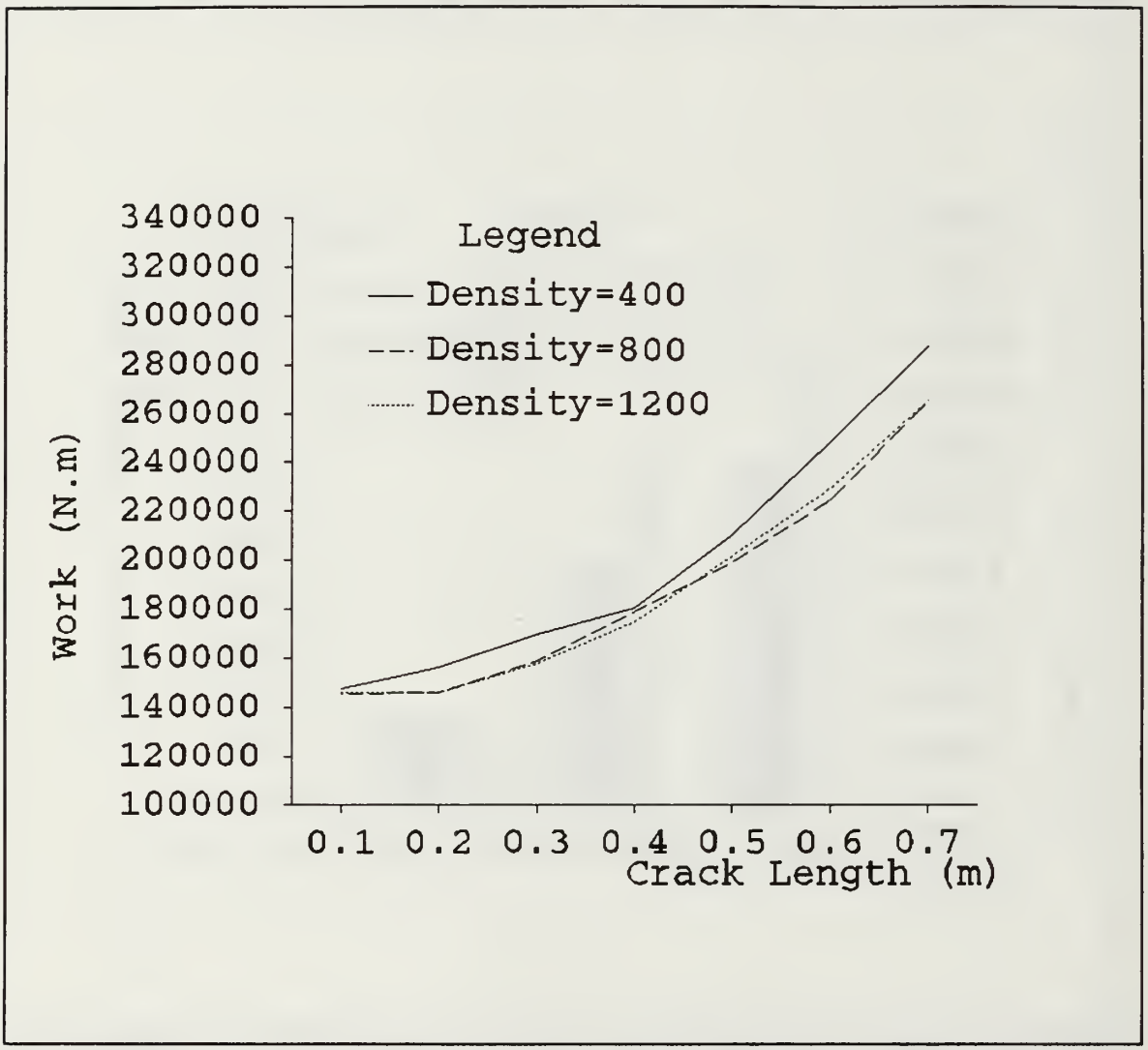

Figure 20 Work Variation for Different Material Densities and Fixed Elastic Modulus Ratio and Crack Velocity

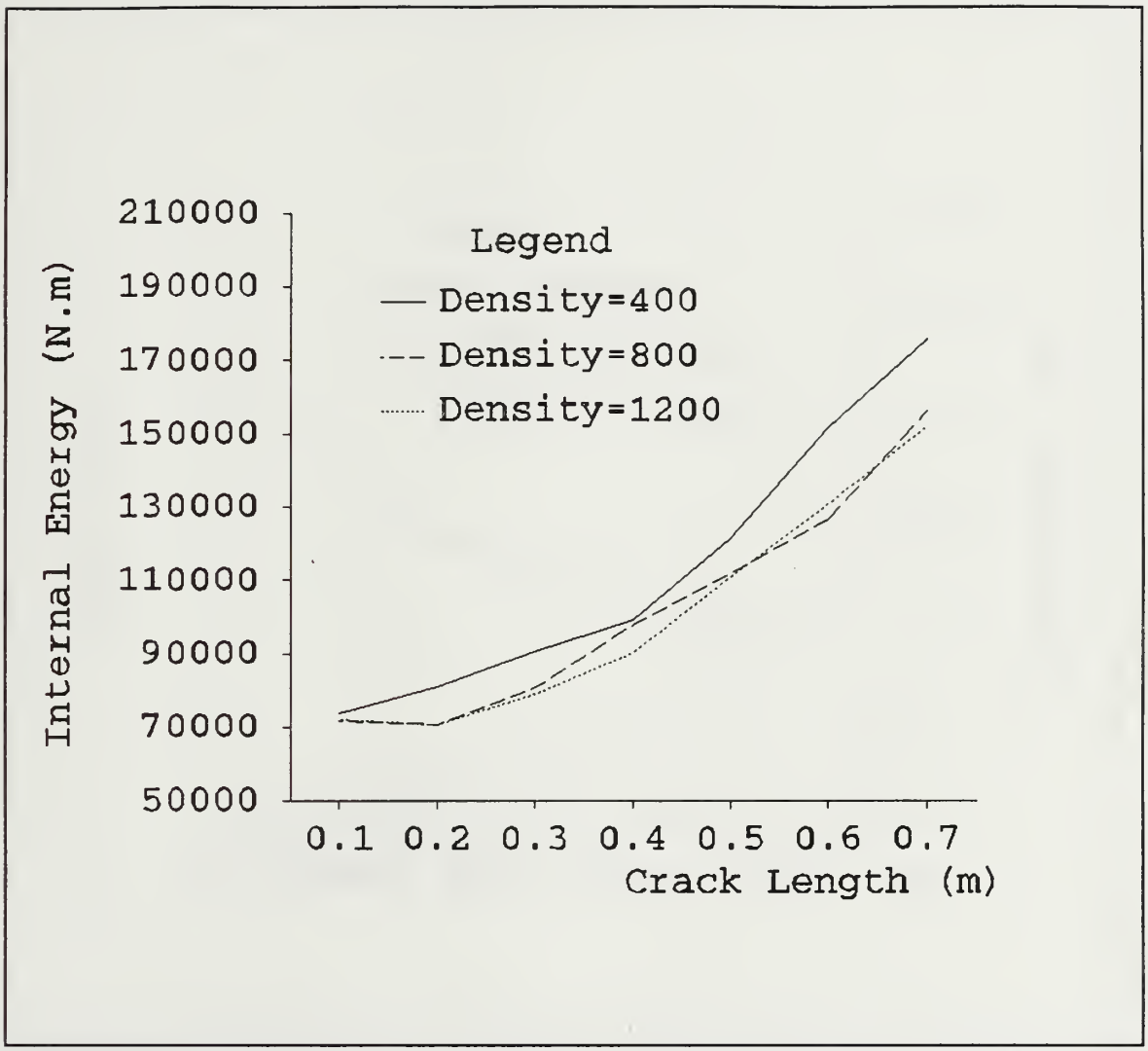

Figure 21 Internal Energy Variation for Different Material Densities and Fixed Elastic Modulus Ratio and Crack Velocity

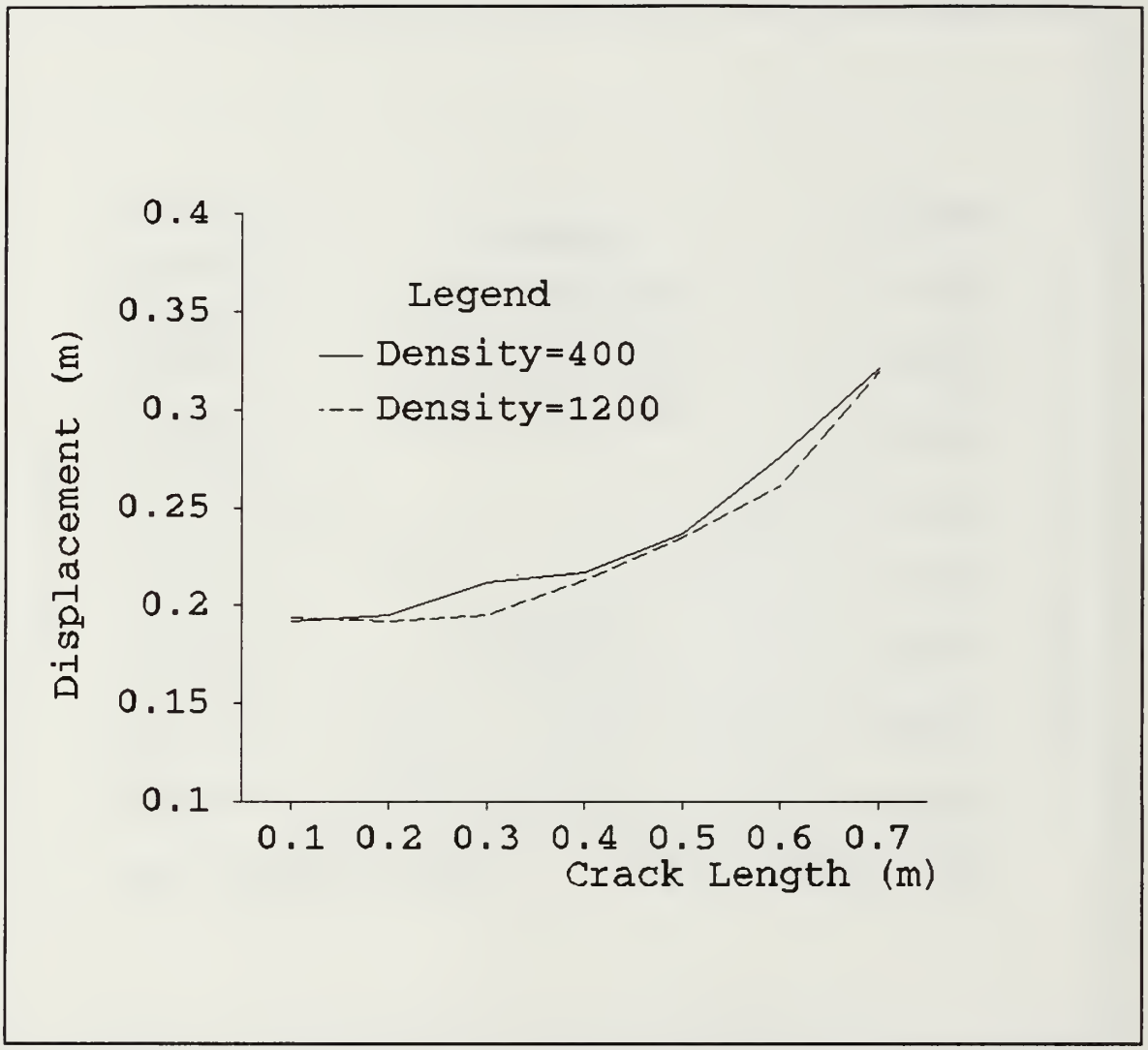

Figure 22 Displacement Values for Different Material Densities and Fixed Elastic Modulus Ratio and Crack Velocity

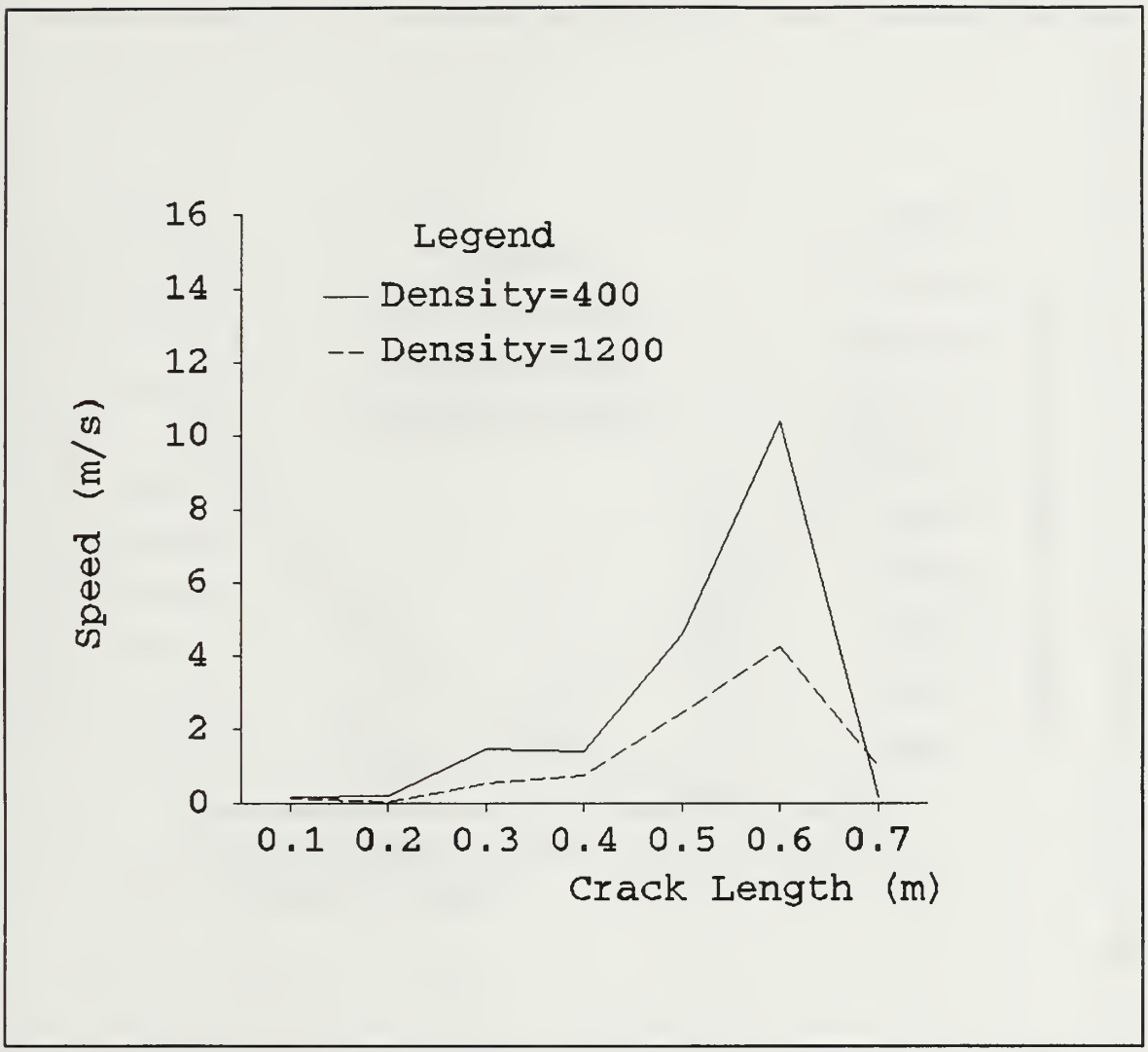

Figure 23 Speed Values for Different Material Densities and Fixed Elastic Modulus Ratio and Crack Velocity

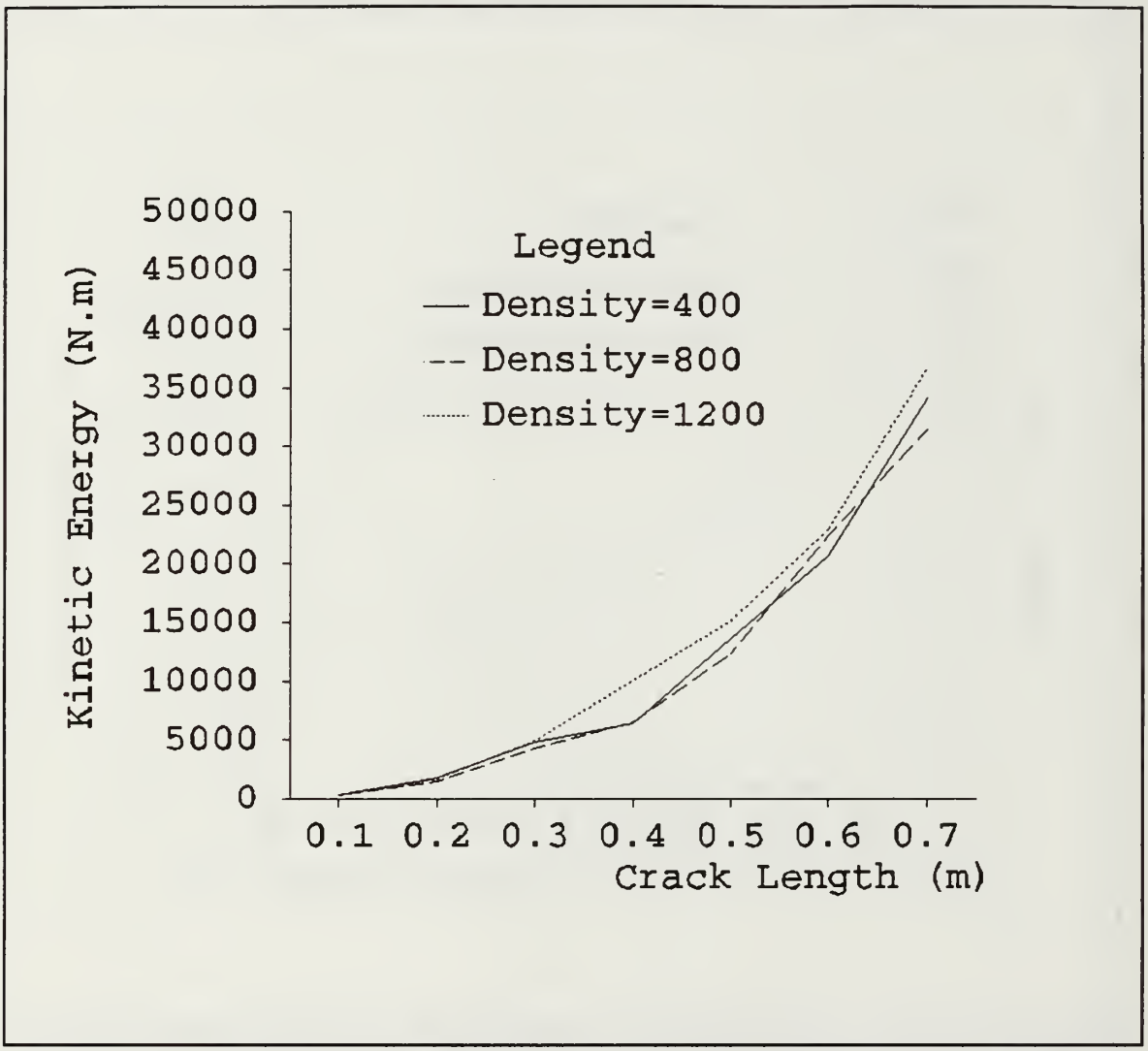

Figure 24 Kinetic Energy Variation for Different Material Densities and Fixed Elastic Modulus Ratio and Crack Velocity

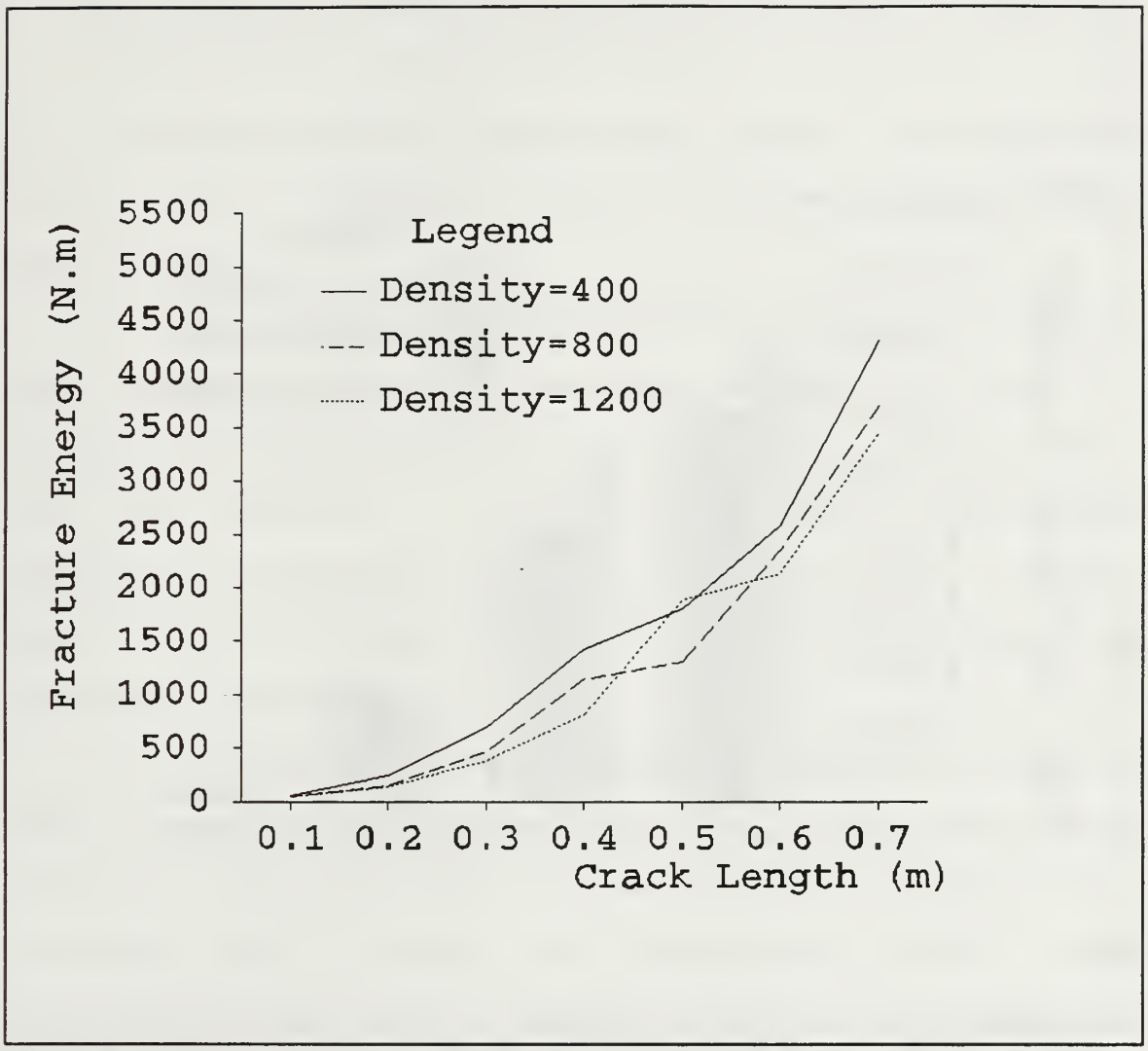

Figure 25 Fracture Energy Variation for Different Material Densities and Fixed Elastic Modulus Ratio and Crack Velocity

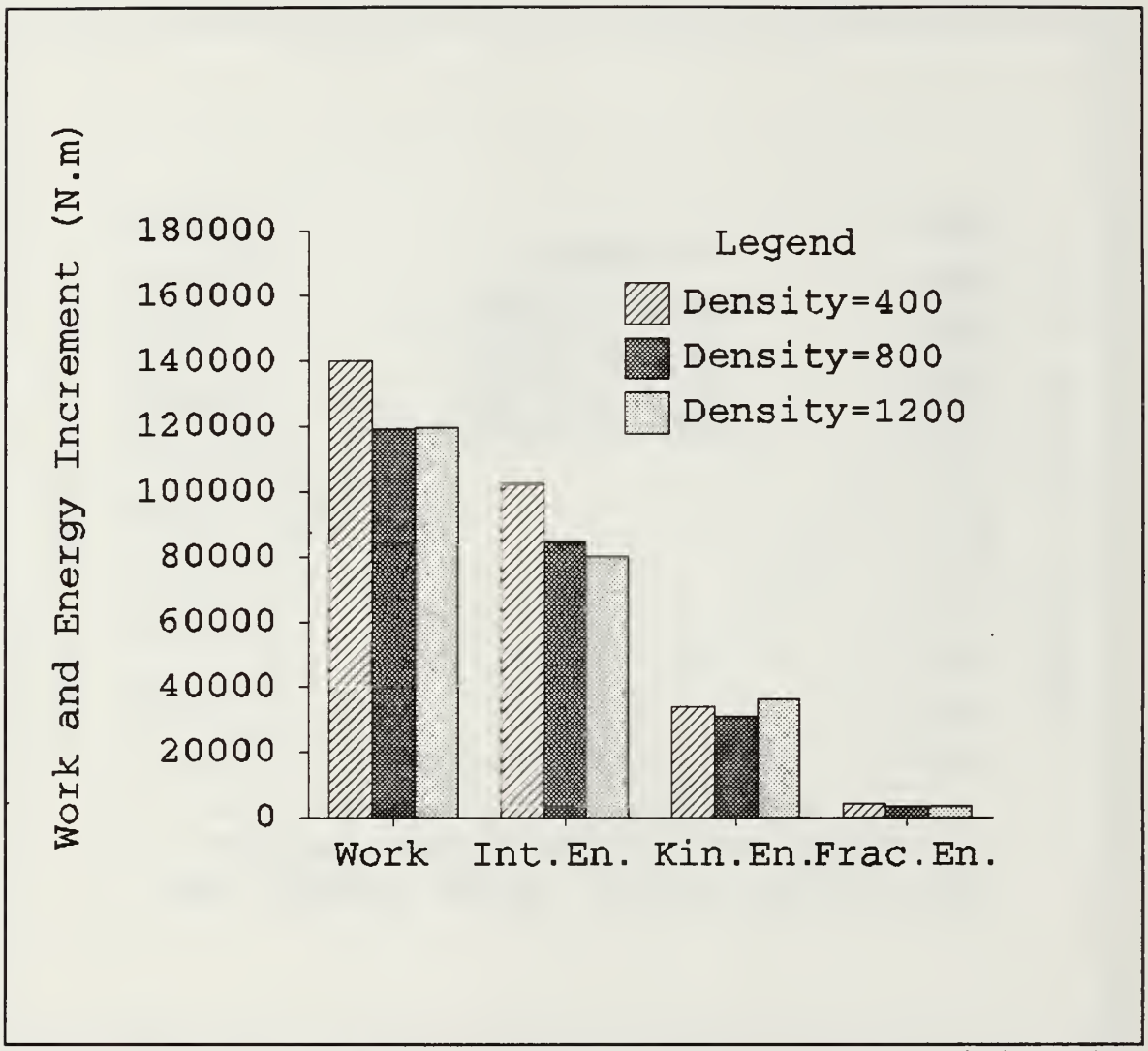

Figure 26 Work and Energy Differences Between the Initial Time and a Late Time for Different Material Densities and Fixed Elastic Modulus Ratio and Crack Velocity

IV. CONCLUSIONS AND RECOMMENDATIONS

The developed computer code has been proven to work well for dynamic crack problems. Very good agreements were obtained for the known solutions. The parametric study of dynamic crack propagation in composite plates provided the following conclusions.

A softer composite plate which has a lower elastic modulus ratio showed a higher fracture energy if the crack velocity, the material density and other characteristics of the problem were held constant. A composite plate with a lower crack velocity and a composite plate with a lower density showed a higher fracture energy provided all other parameters were held constant, respectively.

In this study a discontinuous crack release technique was used to model the crack propagation. This causes sudden shock waves which in turn result in oscillations in solutions. A technique that releases the propagating crack nodes continuously, for example as shown in Ref. 12, is recommended to achieve more stable solutions.

LIST OF REFERENCES

1. Chen, Y.M., "Numerical Computation of Dynamic Stress Intensity Factors by a Lagrangian Finite-Difference Method (The HEMP code)", Engineering Fracture Mechanics, Vol.7, pp.653-660, 1975

2. Kanninen, M.F.,"A Critical Appraisal of Solutions in Dynamic Fracture Mechanics", Numerical Methods in Fracture Mechanics, pp.613-633, 1977

3. Kobayashi, A.S., Mall, S., Urabe, Y., and Emery, A.F., "A Numerical Dynamic Fracture Analysis of Three Wedge-loaded DCB Specimens", Numerical Methods in Fracture Mechanics,pp.673-684, 1977

4. Mall, S., "Dynamic Finite Element Analysis Of Cracked Bodies with Stationary Cracks", Fracture Mechanics: Twelfth Conference, ASTM STP 700, American Society for Testing and Materials, pp.453-465, 1980

5. King,W.W., and Malluck, J.F., "Toward a Singular Element For Propagating Cracks", International Journal of Fracture 14, pp.R7-R11, 1978

6. Ahmad, J., Jung, J., Barnes, C.R., and Kanninen, M.F., "Elastic-Plastic Finite Element Analysis of Dynamic Fracture", Engineering Fracture Mechanics, Vol.17, No.3, pp.235-246, 1983

7. Kishimoto, K., Aoki, S., and Sakata, M., "On the Path Independent Integral-$\hat{J}$", Engineering Fracture Mechanics, Vol.13, pp.841-850, 1980

8. Williams, J.G., Fracture Mechanics of Anisotropic Materials, Application of Fracture Mechanics to Composite Materials, Vol.6, pp.3-38, 1989

9. Sih, G.C., Dynamics of Composites with Cracks, Failure Mechanics of Composites, Vol.3, pp.127-176, 1985

10. Wagner, H.Daniel, Statistical Concepts in the study of Fracture Properties of Fibres and Composites, Application of Fracture Mechanics to Composite Materials, Vol.6, pp.39-77, 1989

11. Jones, R.M., Mechanics of Composite Materials, Scripta Book Co., pp.2-10, 1975

12. Kwon, Y.W., and Akin, J.E., "Development of a Derivative Singular Element for Application to Crack Problems", Computers and Structures, Vol.31, No.3, pp.467-471, 1989

APPENDIX

The general stiffness matrix using a bilinear rectangular element and the general case of material property [D] matrix, that is,

$$[D] = \begin{bmatrix} D_{11} & D_{12} & D_{13} \\ D_{21} & D_{22} & D_{23} \\ D_{31} & D_{32} & D_{33} \end{bmatrix}$$

is given as below:

$$[K] = \begin{bmatrix} K_{11} & K_{12} & K_{13} & K_{14} & K_{15} & K_{16} & K_{17} & K_{18} \\ K_{21} & K_{22} & K_{23} & K_{24} & K_{25} & K_{26} & K_{27} & K_{28} \\ K_{31} & K_{32} & K_{33} & K_{34} & K_{35} & K_{36} & K_{37} & K_{38} \\ K_{41} & K_{42} & K_{43} & K_{44} & K_{45} & K_{46} & K_{47} & K_{48} \\ K_{51} & K_{52} & K_{53} & K_{54} & K_{55} & K_{56} & K_{57} & K_{58} \\ K_{61} & K_{62} & K_{63} & K_{64} & K_{65} & K_{66} & K_{67} & K_{68} \\ K_{71} & K_{72} & K_{73} & K_{74} & K_{75} & K_{76} & K_{77} & K_{78} \\ K_{81} & K_{82} & K_{83} & K_{84} & K_{85} & K_{86} & K_{87} & K_{88} \end{bmatrix}$$

where

$$K_{11} = \frac{16}{3} D_{11} bc^3 + 4 (D_{31} + D_{13}) b^2 c^2 + \frac{16}{3} D_{33} b^3 c$$

$$K_{12} = \frac{16}{3} D_{13} bc^3 + 4 (D_{12} + D_{33}) b^2 c^2 + \frac{16}{3} D_{32} b^3 c$$

$$K_{13} = -\frac{16}{3} D_{11} bc^3 + 4 (-D_{31} + D_{13}) b^2 c^2 + \frac{8}{3} D_{33} b^3 c$$

$$K_{14} = -\frac{16}{3} D_{13} bc^3 + 4 (D_{12} - D_{33}) b^2 c^2 + \frac{8}{3} D_{32} b^3 c$$

$$K_{15} = -\frac{8}{3} D_{11} bc^3 + 4 (-D_{31} - D_{13}) b^2 c^2 - \frac{8}{3} D_{33} b^3 c$$

$$K_{16} = -\frac{8}{3} D_{13} bc^3 + 4 (-D_{12} - D_{33}) b^2 c^2 - \frac{8}{3} D_{32} b^3 c$$

$$K_{17} = \frac{8}{3} D_{11} bc^3 + 4 (D_{31} - D_{13}) b^2 c^2 - \frac{16}{3} D_{33} b^3 c$$

$$K_{18} = \frac{8}{3} D_{13} bc^3 + 4 (-D_{12} + D_{33}) b^2 c^2 - \frac{16}{3} D_{32} b^3 c$$

$$K_{21} = \frac{16}{3} D_{31} bc^3 + 4 (D_{21} + D_{33}) b^2 c^2 + \frac{16}{3} D_{23} b^3 c$$

$$K_{22} = \frac{16}{3} D_{33} bc^3 + 4 (D_{32} + D_{23}) b^2 c^2 + \frac{16}{3} D_{22} b^3 c$$

$$K_{23}=-\frac{16}{3}D_{31}bc^3+4\left(-D_{21}+D_{33}\right)b^2c^2+\frac{8}{3}D_{23}b^3c$$

$$K_{24}=-\frac{16}{3}D_{33}bc^3+4\left(D_{32}-D_{23}\right)b^2c^2+\frac{8}{3}D_{22}b^3c$$

$$K_{25}=-\frac{8}{3}D_{31}bc^3+4\left(-D_{21}-D_{33}\right)b^2c^2-\frac{8}{3}D_{23}b^3c$$

$$K_{26}=-\frac{8}{3}D_{33}bc^3+4\left(-D_{32}-D_{23}\right)b^2c^2-\frac{8}{3}D_{22}b^3c$$

$$K_{27}=\frac{8}{3}D_{31}bc^3+4\left(D_{21}-D_{33}\right)b^2c^2-\frac{16}{3}D_{23}b^3c$$

$$K_{28}=\frac{8}{3}D_{33}bc^3+4\left(-D_{32}+D_{23}\right)b^2c^2-\frac{16}{3}D_{22}b^3c$$

$$K_{31}=-\frac{16}{3}D_{11}bc^3+4\left(D_{31}-D_{13}\right)b^2c^2+\frac{8}{3}D_{33}b^3c$$

$$K_{32}=\frac{16}{3}D_{13}bc^3+4\left(-D_{12}+D_{33}\right)b^2c^2+\frac{8}{3}D_{32}b^3c$$

$$K_{33}=\frac{16}{3}D_{11}bc^3+4\left(-D_{31}-D_{13}\right)b^2c^2+\frac{16}{3}D_{33}b^3c$$

$$K_{34} = \frac{16}{3} D_{13} bc^3 + 4 \left(-D_{12} - D_{33} \right) b^2 c^2 + \frac{16}{3} D_{32} b^3 c$$

$$K_{35} = \frac{8}{3} D_{11} bc^3 + 4 \left(-D_{31} + D_{13} \right) b^2 c^2 - \frac{16}{3} D_{33} b^3 c$$

$$K_{36} = \frac{8}{3} D_{13} bc^3 + 4 \left(D_{12} - D_{33} \right) b^2 c^2 - \frac{16}{3} D_{32} b^3 c$$

$$K_{37} = -\frac{8}{3} D_{11} bc^3 + 4 \left(D_{31} + D_{13} \right) b^2 c^2 - \frac{8}{3} D_{33} b^3 c$$

$$K_{38} = -\frac{8}{3} D_{13} bc^3 + 4 \left(D_{12} + D_{33} \right) b^2 c^2 - \frac{8}{3} D_{32} b^3 c$$

$$K_{41} = -\frac{16}{3} D_{31} bc^3 + 4 \left(D_{21} - D_{33} \right) b^2 c^2 + \frac{8}{3} D_{23} b^3 c$$

$$K_{42} = -\frac{16}{3} D_{33} bc^3 + 4 \left(-D_{32} + D_{23} \right) b^2 c^2 + \frac{8}{3} D_{22} b^3 c$$

$$K_{43} = \frac{16}{3} D_{31} bc^3 + 4 \left(-D_{21} - D_{33} \right) b^2 c^2 + \frac{16}{3} D_{23} b^3 c$$

$$K_{44}=\frac{16}{3}D_{33}bc^3+4\left(-D_{32}-D_{23}\right)b^2c^2+\frac{16}{3}D_{22}b^3c$$

$$K_{45}=\frac{8}{3}D_{31}bc^3+4\left(-D_{21}+D_{33}\right)b^2c^2-\frac{16}{3}D_{23}b^3c$$

$$K_{46}=\frac{8}{3}D_{33}bc^3+4\left(D_{32}-D_{23}\right)b^2c^2-\frac{16}{3}D_{22}b^3c$$

$$K_{47}=-\frac{8}{3}D_{31}bc^3+4\left(D_{21}+D_{33}\right)b^2c^2-\frac{8}{3}D_{23}b^3c$$

$$K_{48}=-\frac{8}{3}D_{33}bc^3+4\left(D_{32}+D_{23}\right)b^2c^2-\frac{8}{3}D_{22}b^3c$$

$$K_{51}=-\frac{8}{3}D_{11}bc^3+4\left(-D_{31}-D_{13}\right)b^2c^2-\frac{8}{3}D_{33}b^3c$$

$$K_{52}=-\frac{8}{3}D_{13}bc^3+4\left(-D_{12}-D_{33}\right)b^2c^2-\frac{8}{3}D_{32}b^3c$$

$$K_{53}=\frac{8}{3}D_{11}bc^3+4\left(D_{31}-D_{13}\right)b^2c^2-\frac{16}{3}D_{33}b^3c$$

$$K_{54} = \frac{8}{3} D_{13} bc^3 + 4 \left(-D_{12} + D_{33} \right) b^2 c^2 - \frac{16}{3} D_{32} b^3 c$$

$$K_{55} = \frac{16}{3} D_{11} bc^3 + 4 \left(D_{31} + D_{13} \right) b^2 c^2 + \frac{16}{3} D_{33} b^3 c$$

$$K_{56} = \frac{16}{3} D_{13} bc^3 + 4 \left(D_{12} + D_{33} \right) b^2 c^2 + \frac{16}{3} D_{32} b^3 c$$

$$K_{57} = -\frac{16}{3} D_{11} bc^3 + 4 \left(-D_{31} + D_{13} \right) b^2 c^2 + \frac{16}{3} D_{33} b^3 c$$

$$K_{58} = -\frac{16}{3} D_{13} bc^3 + 4 \left(D_{12} - D_{33} \right) b^2 c^2 + \frac{8}{3} D_{32} b^3 c$$

$$K_{61} = -\frac{8}{3} D_{31} bc^3 + 4 \left(-D_{21} - D_{33} \right) b^2 c^2 - \frac{8}{3} D_{23} b^3 c$$

$$K_{62} = -\frac{8}{3} D_{33} bc^3 + 4 \left(-D_{32} - D_{23} \right) b^2 c^2 - \frac{8}{3} D_{22} b^3 c$$

$$K_{63} = \frac{8}{3} D_{31} bc^3 + 4 \left(D_{21} - D_{33} \right) b^2 c^2 - \frac{16}{3} D_{23} b^3 c$$

$$K_{64} = \frac{8}{3} D_{33} bc^3 + 4 (-D_{32} + D_{23}) b^2 c^2 - \frac{16}{3} D_{22} b^3 c$$

$$K_{65} = \frac{16}{3} D_{31} bc^3 + 4 (D_{21} + D_{33}) b^2 c^2 + \frac{16}{3} D_{23} b^3 c$$

$$K_{66} = \frac{16}{3} D_{33} bc^3 + 4 (D_{32} + D_{23}) b^2 c^2 + \frac{16}{3} D_{22} b^3 c$$

$$K_{67} = -\frac{16}{3} D_{31} bc^3 + 4 (-D_{21} + D_{33}) b^2 c^2 + \frac{16}{3} D_{23} b^3 c$$

$$K_{68} = -\frac{16}{3} D_{33} bc^3 + 4 (D_{32} - D_{23}) b^2 c^2 + \frac{8}{3} D_{22} b^3 c$$

$$K_{71} = \frac{8}{3} D_{11} bc^3 + 4 (-D_{31} + D_{13}) b^2 c^2 - \frac{16}{3} D_{33} b^3 c$$

$$K_{72} = \frac{8}{3} D_{13} bc^3 + 4 (D_{12} - D_{33}) b^2 c^2 - \frac{16}{3} D_{32} b^3 c$$

$$K_{73} = -\frac{8}{3} D_{11} bc^3 + 4 (D_{31} + D_{13}) b^2 c^2 - \frac{8}{3} D_{33} b^3 c$$

$$K_{74}=-\frac{8}{3}D_{13}bc^3+4\,(D_{12}+D_{33})\,b^2c^2-\frac{8}{3}D_{32}b^3c$$

$$K_{75}=-\frac{16}{3}D_{11}bc^3+4\,(D_{31}-D_{13})\,b^2c^2+\frac{8}{3}D_{33}b^3c$$

$$K_{76}=-\frac{16}{3}D_{13}bc^3+4\,(-D_{12}+D_{33})\,b^2c^2+\frac{8}{3}D_{32}b^3c$$

$$K_{77}=\frac{16}{3}D_{11}bc^3+4\,(-D_{31}-D_{13})\,b^2c^2+\frac{8}{3}D_{33}b^3c$$

$$K_{78}=\frac{16}{3}D_{13}bc^3+4\,(-D_{12}-D_{33})\,b^2c^2+\frac{16}{3}D_{32}b^3c$$

$$K_{81}=\frac{8}{3}D_{31}bc^3+4\,(-D_{21}+D_{33})\,b^2c^2-\frac{16}{3}D_{23}b^3c$$

$$K_{82}=\frac{8}{3}D_{33}bc^3+4\,(D_{32}-D_{23})\,b^2c^2-\frac{16}{3}D_{22}b^3c$$

$$K_{83}=-\frac{8}{3}D_{31}bc^3+4\,(D_{21}+D_{33})\,b^2c^2-\frac{8}{3}D_{23}b^3c$$

$$K_{84} = -\frac{8}{3} D_{33} bc^3 + 4 (D_{32} + D_{23}) b^2 c^2 - \frac{8}{3} D_{22} b^3 c$$

$$K_{85} = -\frac{16}{3} D_{31} bc^3 + 4 (D_{21} - D_{33}) b^2 c^2 + \frac{8}{3} D_{23} b^3 c$$

$$K_{86} = -\frac{16}{3} D_{33} bc^3 + 4 (-D_{32} + D_{23}) b^2 c^2 + \frac{8}{3} D_{22} b^3 c$$

$$K_{87} = \frac{16}{3} D_{31} bc^3 + 4 (-D_{21} - D_{33}) b^2 c^2 + \frac{8}{3} D_{23} b^3 c$$

$$K_{88} = \frac{16}{3} D_{33} bc^3 + 4 (-D_{32} - D_{23}) b^2 c^2 + \frac{16}{3} D_{22} b^3 c$$

In this study the [D] matrix for a unidirectional composite material for the plane stress conditions is;

$$[D] = \begin{bmatrix} D_{11} & D_{12} & 0 \\ D_{21} & D_{22} & 0 \\ 0 & 0 & D_{33} \end{bmatrix}$$

and the nonzero elements of the [D] matrix are;

$$D_{11} = \frac{E_1}{1 - \upsilon_{12}\upsilon_{21}}$$

$$D_{22} = \frac{E_2}{1 - \upsilon_{12}\upsilon_{21}}$$

$$D_{12} = D_{21} = \frac{\upsilon_{12}E_2}{1 - \upsilon_{12}\upsilon_{21}} = \frac{\upsilon_{21}E_1}{1 - \upsilon_{12}\upsilon_{21}}$$

$$D_{33} = G_{12}$$

where subscripts 1 and 2 on the right hand side of the equations are the direction of the fibers and the transverse direction, respectively. Substituting these values into the general stiffness matrix gives the stiffness matrix for a unidirectional composite.

INITIAL DISTRIBUTION LIST

		No. of Copies
1.	Defense Technical Information Center Cameron Station Alexandria, Virginia 22304-6145	2
2.	Library, Code 52 Naval Postgraduate School Monterey, California 93943	2
3.	Deniz Harp Okulu Tuzla Istanbul, Turkey	2
4.	Golcuk Tersanesi Komutanligi Golcuk Kocaeli, Turkey	2
5.	Taskizak Tersanesi Komutanligi Kasimpasa Istanbul, Turkey	2
6.	Deniz Kuvvetleri Komutanligi Personel Egitim Daire Baskanligi Bakanliklar Ankara, Turkey	1
7.	Professor Y.W. Kwon, Code ME/Kw Department of Mechanical Engineering Naval Postgraduate School Monterey, California 93943	1
8.	Department Chairman, Code ME/Kk Department of Mechanical Engineering Naval Postgraduate School Monterey, California 93943	1
9.	Naval Engineering Curricular Office (Code 34) Naval Postgraduate School Monterey, CA 93943	1

10. Dr. Rambert F. Jones, Jr. 1
Submarine Structures Division
Code 172, Bldg. 19 Room A236B
David Taylor Research Center
Bethesda, Maryland 20084-5000

11. Erol Babiloglu 1
Tugrul Cad. Demirkol Sokak No. 76/6
Tutunciftlik, Korfez
Kocaeli, Turkey

12. Istanbul Teknik Universitesi 1
Universite Kutuphanesi, Beyazit
Istanbul, Turkey

13. Ortadogu Teknik Universitesi 1
Universite Kutuphanesi
Ankara, Turkey